IKR Publishers

IKR Journal of Multidisciplinary Studies (IKRJMS)
Journal homepage: https://ikrpublishers.com/ikrjms/
Volume-2, Issue-5 (September-October) 2026
OPEN ACCESS
ISSN: 3107-3999 (Online)

From Lime Scrubbing to Magnesium Bisulfite Circulation: A Critical Review of SO_2 Capture, Sulfite Recovery, and Process Intensification

Antonio Clareti Pereira, PhD*
PhD in Chemical Engineering University of São Paulo (USP) Belo Horizonte, Minas Gerais, Brazil

DOI: *10.5281/zenodo.22681179*

ARTICLE INFO

Article history:
Received : 24-08-2026
Accepted : 02-09-2026
Available online : 09-09-2026

Citation: Pereira, A. C. (2026). From Lime Scrubbing to Magnesium Bisulfite Circulation: A Critical Review of SO_2 Capture, Sulfite Recovery, and Process Intensification. *IKR Journal of Multidisciplinary Studies (IKRJMS), 2*(5), 19-42.

ABSTRACT **Original Research Article**

Wet flue-gas desulfurization remains one of the most mature routes for controlling sulfur dioxide, yet conventional calcium-based systems deliberately combine gas absorption, neutralization, oxidation, crystallization, and solids recirculation in a single slurry loop. This integration is robust but couples SO_2 capture to suspended-solids loading, surface nucleation, scaling, erosion, plugging, mist entrainment, and by-product handling. This critical review evaluates whether magnesium chemistry can be reorganized around a different process principle: capture SO_2 predominantly into a low-solids magnesium-bisulfite-rich liquor and transfer neutralization and controlled magnesium-sulfite precipitation to an external reactor. A structured critical-narrative protocol was applied to 103 scientific and technical sources, combining a 2020–23 August 2026 core corpus with six foundational pre-2020 sources recovered by targeted backward searching. Evidence was classified by industrial, pilot, laboratory, modeling, review, or technical-report level. The synthesis integrates gas–liquid mass transfer, aqueous S(IV) speciation, $MgO/Mg(OH)_2$ dissolution, electrolyte thermodynamics, hydrate phase behavior, sulfite oxidation, crystallization, solids separation, industrial gas-cleaning integration, circular by-product pathways, and technology readiness. The central finding is not that magnesium is intrinsically superior to calcium, but that spatially separating absorption from precipitation can create independent control of capture and solids formation. The concept is technically plausible but not yet validated for broad industrial deployment. Its feasibility depends on maintaining the absorber below relevant saturation limits, controlling oxygen-driven oxidation, managing impurities and water balance, and demonstrating stable recycle chemistry under dynamic gas loads. A staged validation program is proposed, ranging from electrolyte model validation and crystallization kinetics to closed-loop pilot operation and techno-economic comparison with the best available calcium and regenerative alternatives.

Keywords: Sulfur Dioxide, Wet Flue-Gas Desulfurization, Magnesium Bisulfite, Magnesium Sulfite, Process Intensification, Crystallization.

Highlights

- Separating SO_2 absorption from sulfite precipitation can decouple gas-transfer and solids-handling objectives.
- Magnesium-bisulfite operation is promising only if absorber chemistry remains below precipitation limits.
- S (IV) oxidation must be treated as a product-pathway decision, not merely as a side reaction.
- Pilot validation should prioritize recycle stability, impurities, mist, scaling, and dynamic metallurgical gas loads.

Graphical Abstract

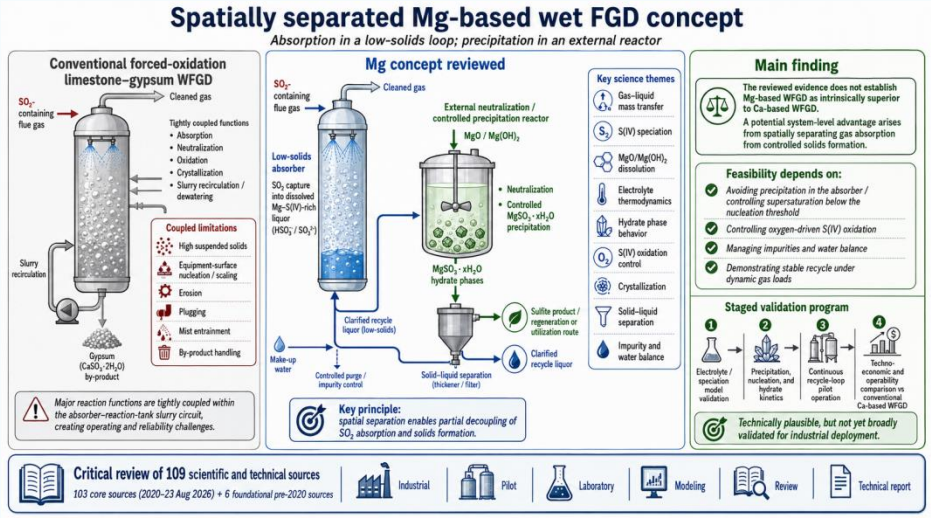

**Corresponding author: Antonio Clareti Pereira, PhD*
PhD in Chemical Engineering University of São Paulo (USP) Belo Horizonte, Minas Gerais, Brazil

Introduction

Industrial context and the persistent SO_2-control problem

Sulfur dioxide control remains a systems problem rather than a single-unit-operation problem. Global inventories continue to identify combustion and mineral-processing chains as major anthropogenic sources, while the relative contribution of individual sectors varies strongly by region, fuel sulfur, concentrate mineralogy, capture infrastructure, and the degree to which sulfur is converted into marketable acid or other products (Zhong et al., 2020; Hu et al., 2026). In non-ferrous metallurgy, the gas can be concentrated enough to justify sulfuric-acid production, but real plants also generate dilute, intermittent, bypass, start-up, converter, furnace, and fugitive streams that do not always match the preferred operating envelope of an acid plant (Liu et al., 2023; Dijkstra et al., 2025; Li et al., 2026; Schmidt & Shang, 2026). This variability is particularly relevant in copper, nickel-copper-PGM, lead-zinc, electric-furnace sulfide, and secondary/e-scrap operations, where off-gas composition and flow can change with furnace mode, feed chemistry, oxygen enrichment, tapping, and downstream gas-cleaning configuration (Hundermark et al., 2026; Strong et al., 2025; Tisdale et al., 2021; Weber et al., 2020; González et al., 2025).

Industrial practice therefore uses a portfolio of sulfur-management routes: direct conversion to sulfuric acid, wet sulfuric acid treatment for leaner gases, regenerative alkali scrubbing, once-through wet FGD, dry or semi-dry sorbents, and hybrid systems. The engineering decision is rarely based on removal efficiency alone; it also depends on gas temperature and humidity, dust and volatile metals, oxygen content, sulfur-load variability, water availability, product market, corrosion, site integration, and the consequences of a temporary loss of capture (Scherman Johansson, 2025; Sun et al., 2021; Zheng et al., 2025; Kumar & Jana, 2022; Xie et al., 2024; Papadopoulos et al., 2022). Recent smelter and gas-cleaning studies reinforce the view that the sulfur-control train must be designed in concert with upstream cooling and particulate removal, rather than appended as an isolated polishing step (Strong et al., 2025; González et al., 2025; Weber et al., 2020).

Why conventional WFGD is simultaneously mature and operationally burdensome

Calcium-based wet FGD is mature because limestone and lime are widely available, chemically effective, and supported by decades of equipment and by-product-management experience. Its maturity, however, should not be confused with the absence of process penalties. The absorber usually operates as a slurry reactor in which dissolution, acid-base neutralization, sulfite formation, oxidation, gypsum crystallization, solids recirculation, and mist generation coexist. Improvements in spray-tower design and sorbent reactivity can increase transfer rates, yet they do not eliminate the fundamental coupling between gas absorption and solids generation (Ghosh et al., 2026; França et al., 2020; Stanienda-Pilecki, 2021; Tang et al., 2024). Scale formation remains a persistent cross-industry wet-scrubber problem because local supersaturation, wall wetting, temperature gradients, hard-water species, and deposition can create operating conditions that differ markedly from bulk-tank averages (Fungene et al., 2023).

Historical full-scale evidence is important when judging alternatives. A 1970s coal-fired demonstration of magnesia scrubbing treated flue gas from half of a 190-MW unit firing 3.5% sulfur coal, achieved approximately 90% SO_2 removal over about 2,800 h of logged operation, and successfully

regenerated and recycled magnesia (Koehler, 1977). The later U.S. EPA technology summary documented multi-year operation of early MgO-FGD installations and emphasized that the process was technically feasible but more complex than once-through calcium scrubbing (U.S. Environmental Protection Agency, 1981).

Magnesium systems deserve renewed attention because MgO and $Mg(OH)_2$ combine acid-neutralization capacity with chemistry that can support highly soluble bisulfite species over part of the operating pH range. The literature spans MgO reactivity and particle-size effects, hydroxylation and brucite dispersion, sulfite oxidation, regeneration, and by-product recovery (Bakhshi Ani & Ale Ebrahim, 2020; Bakhshi Ani & Ale Ebrahim, 2021a; Bakhshi Ani & Ale Ebrahim, 2021b; Bassioni et al., 2021; Cao & Zhang, 2020; Ma et al., 2024; Tang et al., 2020; von Hoessle et al., 2021; H. Wang et al., 2020; Zhao et al., 2025; Zhao & Zou, 2021; Zhu et al., 2026). Yet this literature often treats absorption, oxidation, regeneration, or materials development separately. A critical process question remains underdeveloped: can the absorber itself be operated deliberately as a low-solids bisulfite-circulation device, while precipitation is moved to an external vessel in which supersaturation, seeding, residence time, and solids separation are controlled independently?

Scope, critical-review logic, and contribution

This review evaluates that question by integrating evidence from wet and dry FGD reviews, magnesium absorbent studies, electrolyte-thermodynamic modeling, gas-liquid mass-transfer simulations, sulfite oxidation catalysis, industrial smelter gas treatment, process optimization, and by-product utilization (Hanif et al., 2020; Kumar & Jana, 2022; Xie et al., 2024; Dong et al., 2021). The approach is critical-narrative rather than meta-analytic because the evidence base spans different feed gases, laboratory reactors, industrial systems, thermodynamic models, catalyst studies, and product objectives. Evidence is therefore interpreted according to what it actually demonstrates: industrial operability, pilot feasibility, laboratory mechanism, model prediction, or conceptual integration. The proposed magnesium-bisulfite/external-precipitation configuration is treated as a process hypothesis to be tested, not as an established best available technology.

Table 1 positions the major wet and regenerative sulfur-capture families in relation to the specific process question addressed in this review.

Table 1. *Representative SO_2-Control Routes and the Process Trade-Offs Relevant to Magnesium-Bisulfite Circulation*

Route	Typical absorbing phase / product	Primary strength	Critical limitation
Limestone/lime WFGD	$CaCO_3$/$Ca(OH)_2$ slurry → $CaSO_3$/$CaSO_4$ solids	Mature, low-cost reagent, robust high removal	Solids-intensive absorber; scaling, erosion, gypsum handling
Seawater / alkaline water	Dissolved alkalinity; sulfate discharged or treated	Low reagent requirement where seawater is available	Site-specific water chemistry and discharge constraints
Sodium regenerative	Na-based liquor; SO_2 regenerated	High capture with recoverable concentrated SO_2	Regeneration energy, salt management, process complexity
MgO/$Mg(OH)_2$ WFGD	$Mg(HSO_3)_2$/$MgSO_3$/$MgSO_4$ depending pH and oxidation	High reactivity; potential liquid-phase operation and recovery	Higher Mg cost; oxidation/speciation and solids-path control
Proposed Mg-bisulfite + external precipitation	Low-solids absorber liquor → external $MgSO_3$ precipitation	Decouples gas absorption from solids formation	Requires validated precipitation envelope, recycle stability, and pilot demonstration

Note. Author synthesis adapted from Hanif et al. (2020), Kumar and Jana (2022), Xie et al. (2024), and Zheng et al. (2025).

The comparison in Table 1 makes the central distinction explicit. The proposed configuration is not simply a substitution of $Mg(OH)_2$ for $Ca(OH)_2$. Its value proposition depends on rearranging where solids are allowed to form. If the magnesium circuit is operated as another high-solids slurry scrubber, much of the hydrodynamic argument disappears; if a stable low-solids absorption window can be maintained, absorber design can be optimized around interfacial area and liquid distribution rather than around simultaneous crystallization duty.

Review Methodology and Evidence Classification

Search update, eligibility, and corpus definition

To make the evidence base reproducible without recasting the article as a PRISMA-style systematic review, the literature already assembled for this manuscript was re-screened against a prespecified critical-narrative protocol. The core

corpus comprised 97 published sources dated from 2020 through 23 August 2026. Targeted backward searching was then used to recover six pre-2020 sources that are foundational for historical industrial performance of magnesia scrubbing, aqueous S(IV) acid–base chemistry, magnesium-sulfite hydrate precipitation, regeneration, and mixed Ca–Mg–sulfite–sulfate phase equilibria (Koehler, 1977; Lowell et al., 1977; Neta & Huie, 1985; Yan et al., 2014; Meng et al., 2018; U.S. Environmental Protection Agency, 1981). The resulting evidence base contains 103 sources.

The search update combined publisher and institutional searches across ScienceDirect, ACS Publications, PubMed/PMC, Springer-linked proceedings, and U.S. EPA/NTIS repositories with general scholarly web searching. Search strings were organized around the following concept blocks: (magnesium oxide OR magnesium hydroxide OR magnesia OR brucite) AND (SO_2 OR flue gas desulfurization OR wet scrubbing); magnesium sulfite AND (solubility OR hydrate OR crystallization OR precipitation); magnesium sulfite AND (oxidation OR regeneration); calcium OR limestone WFGD AND (scaling OR gypsum OR benchmark); and metallurgical off-gas AND (SO_2 capture OR acid plant OR smelter). Searches were supplemented by backward citation tracing from recent reviews and thermodynamic studies.

Inclusion, exclusion, and evidence hierarchy

Eligible sources were peer-reviewed research articles, critical reviews, conference proceedings with identifiable industrial process content, and government or institutional technical reports that contributed directly to SO_2 absorption, magnesium reagent dissolution, S(IV) speciation, phase equilibrium, precipitation/crystallization, oxidation, solids separation, industrial operability, environmental performance, or process economics. Preprints without a final publication, duplicate records, promotional material, patents used only for priority claims, and studies in which SO_2 capture was incidental were excluded. No quantitative meta-analysis was attempted because reactor geometry, inlet SO_2, gas composition, reagent form, L/G ratio, temperature, pH, oxidation state, duration, and reporting metrics are too heterogeneous for a common effect size.

Evidence was interpreted hierarchically by what it can support: industrial/full-scale operation for availability and operability claims; pilot evidence for integrated recycle and transient response; laboratory studies for mechanism, kinetics, and materials behavior; thermodynamic or CFD/process models for predicted operating envelopes; and reviews for contextual synthesis. This hierarchy is used explicitly to avoid treating high laboratory removal efficiency or catalyst activity as proof of industrial readiness.

Representative quantitative evidence

Table 2 provides a quantitative evidence matrix for representative studies that directly constrain the proposed low-solids magnesium-bisulfite/external-precipitation architecture. The table is not a meta-analysis; its purpose is to expose the scale, measured variable, and transferability of the evidence rather than to average non-equivalent experiments.

Table 2. *Representative Quantitative Evidence Relevant to Magnesium-Based SO_2 Capture*

Study/scale	Representative quantitative evidence	Design relevance	Transferability limit
Koehler (1977) — full scale	50% of a 190-MW unit; 3.5% S coal; ~90% SO_2 removal; ~2,800 h; MgO regenerated/recycled.	Industrial feasibility of MgO capture and recycle.	Historical slurry architecture, not the proposed low-solids loop.
Lowell et al. (1977). — precipitation	$MgSO_3 \cdot 6H_2O$ forms in tens of minutes; dissolution/trihydrate formation requires hundreds of minutes; equilibrium can require thousands.	Residence time and seed phase control are intrinsic to $MgSO_3$ recovery.	Simplified electrolyte versus impurity-rich recycle.
Meng et al. (2018). — phase equilibrium	At 298.15 K, five crystallization fields were mapped in Ca^{2+}/Mg^{2+}–SO_3^{2-}/SO_4^{2-}–H_2O, including $MgSO_3 \cdot 6H_2O$ and $MgSO_4 \cdot 7H_2O$.	Competing Ca–Mg–sulfite–sulfate phase fields matter.	Single temperature; no gas-phase coupling.
Zhao & Zou (2021). — absorption	Mass-transfer coefficient up to 2.302 mmol m^{-2} s^{-1} kPa^{-1} at 5 wt%; improvement diminished above ~4 wt%.	Particle size/suspension properties alter apparent capture.	Nanofluid preparation may not transfer economically.
Tian et al. (2021) — regeneration	Sulfur-assisted regeneration reduced required temperature from >950 to ~650 °C; SO_2 ~20 vol% at 750 °C; E_a 76.51 kJ mol^{-1}.	Regeneration can recover MgO and concentrated SO_2.	High-temperature step; not direct crystallizer evidence.
Ma et al. (2024) — dissolution	Modified 5 wt% MgO: ζ-potential >50 mV after 30 d; sedimentation ≤7%; micron MgO dissolution ~700 min; k = 0.00084–0.0030 min^{-1}.	Alkalinity release depends on dispersion and particle properties.	Laboratory preparation and chemistry.

Note. Values are reported as given by the cited sources and should not be interpreted as directly comparable because gas composition, reactor design, reagent preparation, and test duration differ.

Fundamentals of SO_2 Absorption

Gas-liquid mass transfer and chemical enhancement

SO_2 absorption is governed by gas-side transport, interfacial equilibrium, liquid-side transport, and rapid aqueous reactions that consume dissolved SO_2, thereby maintaining a concentration driving force. Spray towers, packed or structured contactors, venturi devices, and hybrid scrubbers differ principally in how they create interfacial area and renew liquid films. Modeling studies of WFGD show that gas velocity, liquid-to-gas ratio, droplet size, absorber height, reagent alkalinity, and reaction kinetics interact rather than act independently (Liu et al., 2025; Zhao et al., 2021; Wilailak et al., 2021; Zhao, Zhang, et al., 2022). This is why a reagent with favorable equilibrium chemistry can still perform poorly if slurry rheology, nozzle fouling, liquid maldistribution, or mass-transfer resistance limits access to that chemistry.

For a reactive alkaline liquid, the two-film model is most useful when interpreted qualitatively: SO_2 crosses the gas film, dissolves at the interface, and is rapidly converted into bisulfite and sulfite as alkalinity is supplied. The faster this conversion relative to molecular diffusion, the lower the dissolved molecular SO_2 concentration in the liquid film and the larger the effective driving force. MgO/$Mg(OH)_2$ systems add another kinetic layer because alkalinity supply depends on solid dissolution or hydroxide availability; microstructure, hydration history, particle size, and dispersion therefore influence the apparent absorption kinetics (Ma et al., 2024; Tang et al., 2020; von Hoessle et al., 2021; Zhao & Zou, 2021; Zhu et al., 2026; Bassioni et al., 2021). Surface studies further show that adsorption and oxidation can occur directly on MgO-derived surfaces, which complicates attempts to reduce the system to a single homogeneous reaction (H. Wang et al., 2020).

Figure 1 is inserted here to connect absorber pH with the aqueous S(IV) species that create or remove the liquid-phase driving force.

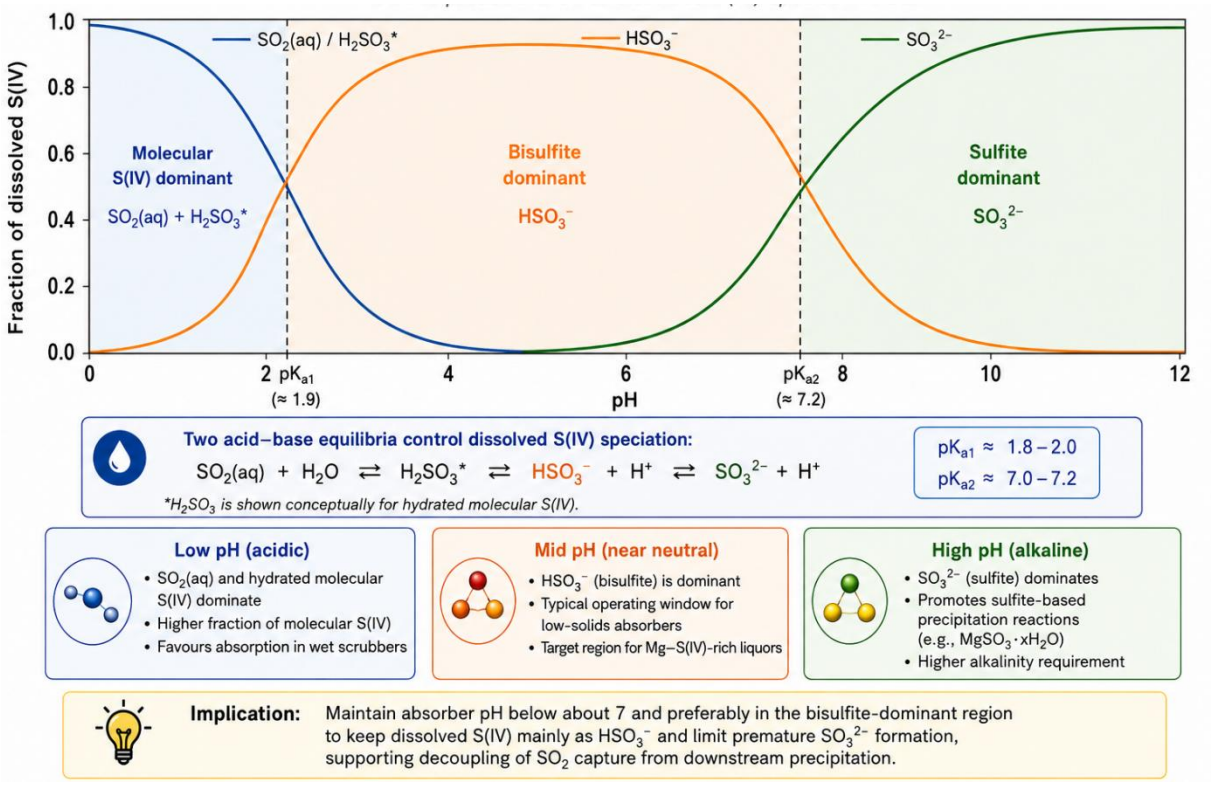

Figure 1. *Aqueous S(IV) Speciation as a Function of pH*

Note. Calculated from diprotic-acid distribution equations using representative $pKa_1 \approx 1.86$ and $pKa_2 \approx 7.2$ values near ambient conditions (Neta & Huie, 1985); author synthesis adapted conceptually from SO_2-absorption chemistry discussed by Kumar and Jana (2022), Xie et al. (2024), and Zhong et al. (2026).

As Figure 1 shows, bisulfite dominates a broad intermediate-pH region, whereas sulfite becomes important as pH rises. That shift matters operationally. A strongly alkaline absorber maximizes instantaneous chemical absorption but also moves the liquid toward sulfite-rich conditions in which magnesium-sulfite saturation may become relevant. A more acidic bisulfite-rich absorber can preserve a large dissolved S(IV) inventory with less tendency toward sulfite precipitation, provided sufficient neutralization capacity is restored elsewhere in the circuit. This is the thermodynamic basis for spatially separating capture from precipitation.

Dissolution, alkalinity supply, and the role of magnesium solids

Magnesium reagent quality is not a secondary detail. Acetic-acid-treated MgO, caustic-magnesia hydration, particle-size control, hydration additives, and tailored $Mg(OH)_2$ morphology have all been studied because dissolution and hydration determine how rapidly solid reagent can replenish alkalinity (Bakhshi Ani & Ale Ebrahim, 2020; Bassioni et al., 2021; Ma et al., 2024; Tang et al., 2020; Zhao & Zou, 2021; Zhu et al., 2026). Natural brucite dispersion adds another scale-up issue: even a chemically reactive solid can settle, agglomerate, or feed non-uniformly if suspension stability is inadequate (Zhao et al., 2025). Thus a proposed low-solids absorber should not be interpreted as a solids-free plant; rather, the design objective is to keep the absorption contactor itself low in suspended crystallized product while handling reagent dissolution and precipitation in dedicated equipment.

Dry and fixed-bed studies of MgO demonstrate strong intrinsic affinity for SO_2 and clarify solid-gas reaction mechanisms, but their kinetics cannot be transferred directly to a wet circulation loop (Bakhshi Ani & Ale Ebrahim, 2021a; Bakhshi Ani & Ale Ebrahim, 2021b; Cao & Zhang, 2020; He et al., 2025; N. Zhang et al., 2025). In wet service, dissolution, liquid-phase speciation, droplet hydrodynamics, and oxygen transfer dominate. The fixed-bed literature is nevertheless useful because it shows how reactivity depends on surface state and because it reinforces a broader point: magnesium chemistry is highly sensitive to how the reagent is manufactured and conditioned.

Impurity chemistry and co-pollutant interactions

Real metallurgical gases contain more than SO_2. SO_3, acid mist, halides, arsenic, mercury, selenium, and fine particulate matter can alter alkalinity consumption, nucleation, corrosion, and product purity. Studies of SO_3 uptake by alkaline absorbents and simultaneous pollutant removal show that absorbent chemistry can be leveraged for co-control but can also introduce new ionic loads (Guo et al., 2025; Liang et al., 2022; Y. Wang et al., 2020; Xing et al., 2022; Zhang et al., 2021). Copper-smelter slag slurries, tailings-based absorption, manganese ores, and calcine oxides have been investigated as reactive sorbents or integrated resource-recovery media (Bao et al., 2021; Tao et al., 2022; Tang et al., 2023; Weng et al., 2023). These routes broaden the circular-economy opportunity but also emphasize why a magnesium-bisulfite circuit must be tested with representative impurities rather than synthetic SO_2–air mixtures alone.

Conventional Calcium-Based Scrubbing as the Benchmark

Chemistry and process configuration

A conventional limestone or lime WFGD system intentionally combines gas absorption with neutralization and, in forced-oxidation configurations, conversion of calcium sulfite to gypsum. Limestone dissolution supplies alkalinity more slowly than lime but at lower reagent cost, while lime offers faster reaction and can be modified by additives or magnesium-bearing phases (França et al., 2020; Stanienda-Pilecki, 2021; Tang et al., 2024). Modern spray-tower studies continue to optimize absorber height and contacting conditions because large-scale performance remains a balance among mass transfer, reaction, pressure drop, and slurry circulation (Ghosh et al., 2026; Liu et al., 2025).

Figure 2 is included here because the physical locations of oxidation and solids recirculation explain why scaling and mist control are inseparable from absorber operation.

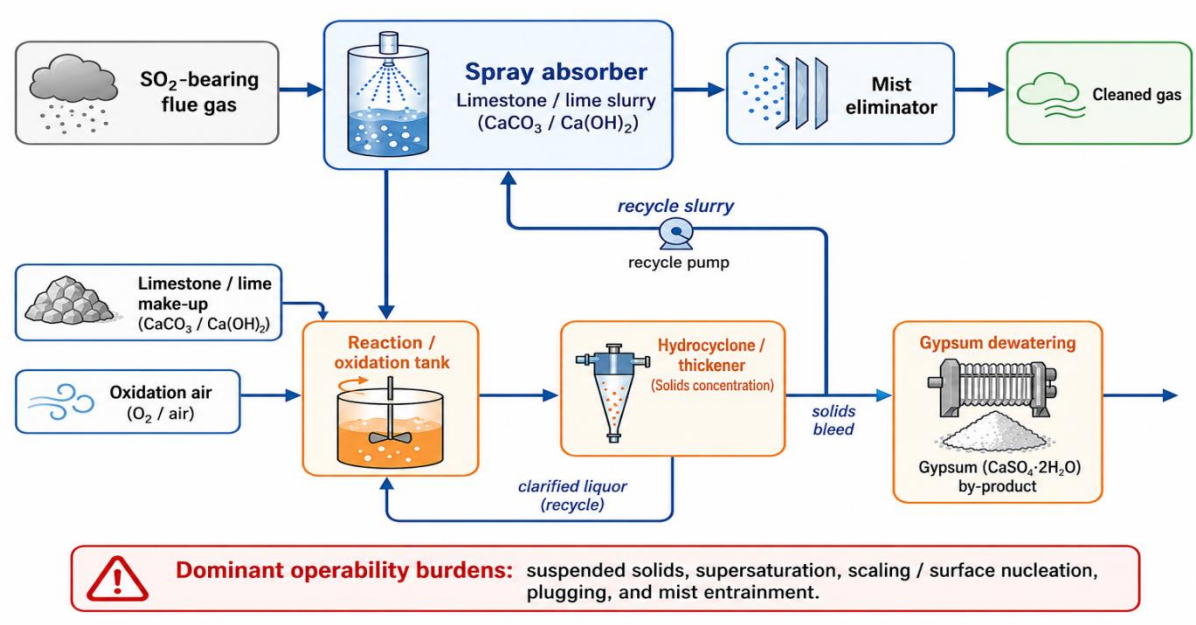

Figure 2. *Simplified Conventional Calcium-Based Wet-FGD Flowsheet*

Note. Author synthesis adapted from the process configurations reviewed by Kumar and Jana (2022), Ghosh et al. (2026), and Xie et al. (2024).

Figure 2 highlights the defining feature of the calcium benchmark: the absorber is part of a circulating slurry loop. This architecture is effective and industrially proven, but it places nozzles, recirculation pumps, absorber walls, internals, and mist eliminators in direct contact with a multiphase liquid whose solids content and supersaturation change continuously. Scale control therefore depends on chemistry, hydrodynamics, wash practice, water quality, and mechanical design at the same time.

Scaling, plugging, erosion, and mist generation

Scale formation in wet scrubbers is caused not only by bulk equilibrium but also by local supersaturation and surface-specific phenomena. Evaporation near gas-liquid interfaces, temperature gradients, stagnant zones, wall films, and hard-water ions can trigger heterogeneous nucleation even when tank chemistry appears acceptable (Fungene et al., 2023). In slurry WFGD, deposited crystals increase roughness and capture more solids, while abrasive circulation accelerates wear. Plugging can then appear in nozzles, small-bore lines, hydrocyclones, and mist-eliminator wash systems. These are maintenance mechanisms rather than mere chemistry curiosities because they reduce available interfacial area and force operators to increase wash water, recirculation, or outage frequency.

Water and heat recovery studies show another consequence of the coupled loop: efforts to cool, dehumidify, or concentrate the scrubber circuit change saturation ratios and water balance (Chen et al., 2020; Zhang et al., 2022). Open- versus closed-loop scrubber strategies in marine service likewise demonstrate that water management and salt accumulation can dominate long-term operation even when short-term SOx removal remains high (Lee et al., 2023). The benchmark lesson is therefore not that calcium WFGD is deficient; it is that its proven performance is purchased through deliberate management of a solids-rich circulating reactor.

Why the calcium benchmark remains difficult to displace

Any alternative must compete against more than reagent price. Calcium systems benefit from mature equipment vendors, well-known materials of construction, established gypsum handling practices, large operating datasets, and familiar control strategies. A magnesium route that saves on cleaning but requires expensive reagents, complex regeneration, impurity-sensitive crystallization, or unreliable product markets may not improve lifecycle costs. Conversely, a site with severe scaling, constrained solids disposal, valuable sulfur recovery, or strong integration with an acid plant may assign a higher economic value to low-solids absorber operation than a generic cost comparison would suggest. This asymmetry is central to the techno-economic analysis developed later in the review.

Thermodynamics of the Mg–SO_2–H_2O System

Aqueous speciation, reagent dissolution, and saturation index

The magnesium system couples MgO/$Mg(OH)_2$ dissolution or hydration, SO_2 hydration and dissociation, magnesium-ion association, possible magnesium-sulfite hydrate precipitation, and oxidation of S(IV) to sulfate. At near-ambient conditions, the aqueous SO_2/HSO_3^- and HSO_3^-/SO_3^{2-} acid–base transitions are commonly represented by $pK_{a1} \approx 1.86$ and $pK_{a2} \approx 7.2$, respectively (Neta & Huie, 1985). These values are useful for orientation but are not plant design constants because temperature and ionic strength alter activities. Thermodynamic process simulations therefore require simultaneous treatment of MgO–CaO–CO_2–SO_2–H_2O–O_2 chemistry and non-ideal activity coefficients (Weiß et al., 2021; Weiß et al., 2023; Weiß & Harasek, 2021).

$$SO_2(aq) + H_2O \rightleftharpoons H^+ + HSO_3^-$$

$$HSO_3^- \rightleftharpoons H^+ + SO_3^{2-}$$

$$MgO(s) + 2H^+ \rightarrow Mg^{2+} + H_2O$$

$$Mg^{2+} + SO_3^{2-} + xH_2O \rightleftharpoons MgSO_3 \cdot xH_2O(s)$$

$$SO_3^{2-} + \tfrac{1}{2}O_2 \rightarrow SO_4^{2-}$$

$$SI = \log_{10}(IAP/Ksp)$$

The saturation index provides a practical control variable: $SI < 0$ indicates undersaturation, $SI = 0$ equilibrium, and $SI > 0$ thermodynamic supersaturation. Because the ion-activity product (IAP) depends on Mg^{2+} and SO_3^{2-} activities rather than concentration alone, pH cannot be used as the sole precipitation-control variable.

At lower pH, absorbed sulfur is predominantly present as dissolved bisulfite; as pH and available Mg^{2+}/alkalinity increase, the sulfite fraction rises and the IAP for magnesium sulfite can approach or exceed Ksp. Mixed magnesium–sodium sulfite systems demonstrate that buffering and ion pairing can stabilize dissolved S(IV) over useful operating windows (Huang et al., 2022; Wang et al., 2023; Zhong et al., 2026). The absorber should therefore be controlled by species distribution and calculated saturation state together with pH. The same pH can represent very different precipitation risk when total Mg, temperature, sulfate, chloride, calcium, sodium, and trace impurities differ.

Magnesium sulfite should not be treated as a single generic solid. Foundational precipitation work showed that $MgSO_3 \cdot 6H_2O$ can form rapidly as a kinetically favored phase, whereas $MgSO_3 \cdot 3H_2O$ can become the thermodynamically stable hydrate over relevant temperature ranges; reported time scales differed by orders of magnitude between initial hexahydrate precipitation, subsequent

dissolution/reprecipitation, and approach to trihydrate equilibrium (Lowell et al., 1977). Modern mixed-electrolyte measurements likewise identify $MgSO_3 \cdot 6H_2O$ and $MgSO_4 \cdot 7H_2O$ as distinct crystallization fields in Ca–Mg–sulfite–sulfate solutions at 298.15 K (Meng et al., 2018). Consequently, phase identity, water of hydration, morphology, particle-size distribution, agglomeration, filtrability, and redissolution history are design variables for the external crystallizer rather than secondary solid-state details.

Phase behavior, hydrate selection, and the precipitation envelope

Figure 3 is inserted here as a conceptual map of the competing chemical regions; it is intentionally not presented as a calculated phase boundary for a specific plant liquor.

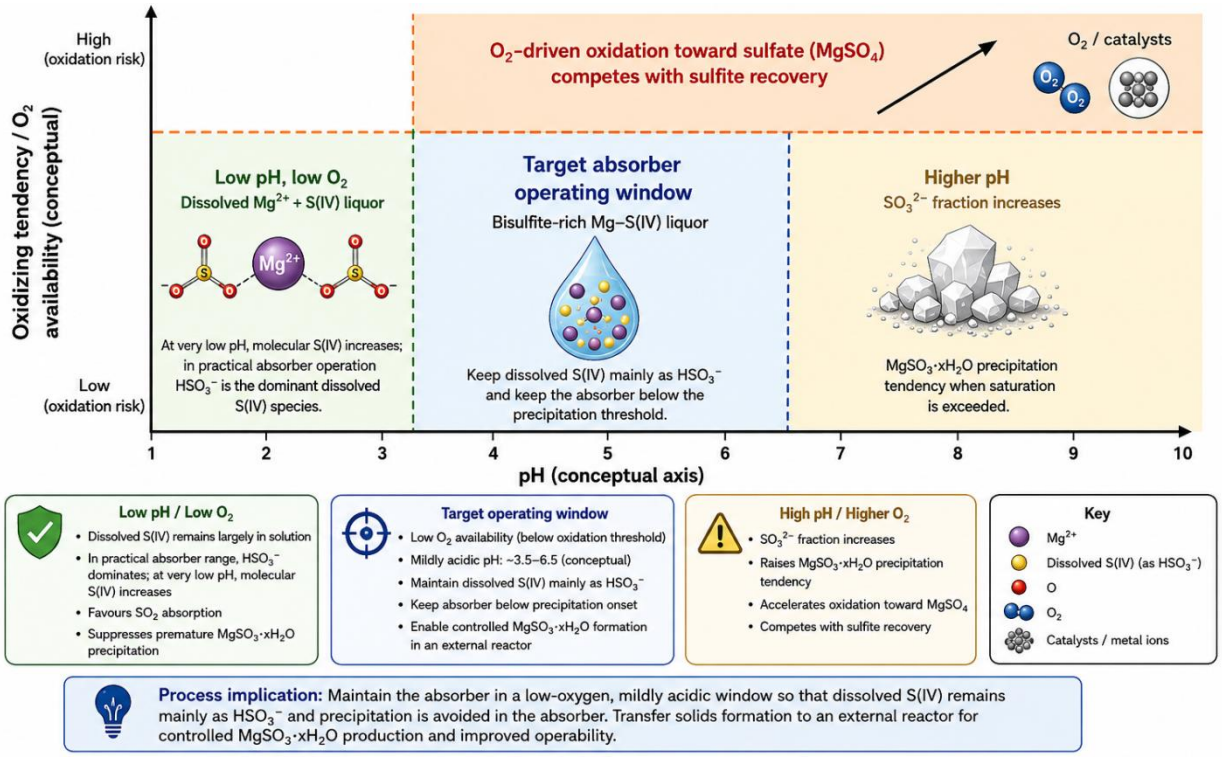

Figure 3. *Conceptual Operating Map for the Mg–S(IV)–O₂–H₂O System*

Note. Author synthesis adapted from thermodynamic and solubility studies by Weiß and Harasek (2021), Weiß et al. (2023), and Zhong et al. (2026). Boundaries are conceptual and must be recalculated for the actual electrolyte composition and temperature.

Figure 3 separates four tendencies that are often conflated. First, acidic-to-intermediate conditions favor a bisulfite-rich dissolved inventory. Second, increasing pH raises the sulfite fraction and can support $MgSO_3$ supersaturation. Third, exceeding the solubility limit introduces nucleation and solids formation. Fourth, oxygen transfer and catalytic surfaces can divert S(IV) toward sulfate. A successful external-precipitation process must exploit the first tendency in the absorber, deliberately enter the third in a separate vessel, and either suppress or intentionally exploit the fourth depending on the desired product.

Oxidation as a thermodynamic and kinetic branch point

Sulfite oxidation is extensively studied because conventional magnesium FGD often aims to produce stable sulfate products or to regenerate the process. Catalysts based on cobalt, manganese, MOFs, supported oxides, activated carbon fibers, and multifunctional materials can greatly accelerate $MgSO_3$ oxidation (Fang et al., 2021; J. Feng et al., 2024; L. Feng et al., 2024; Geng et al., 2023; Li et al., 2020; Li et al., 2025; Meng et al., 2023; Qi et al., 2021; L). Wang et al., 2020; Y. Wang et al., 2020; Xing et al., 2020; Zeng et al., 2025). Other work combines oxidation with capture of arsenic, mercury, lead, selenium, or other contaminants (Liang et al., 2022; Qi et al., 2026; Y. Wang et al., 2020; Xing et al., 2022; Yang et al., 2026; Zhang et al., 2021). Process optimization and hybrid modeling studies likewise treat S(IV) oxidation as a controllable reactor operation rather than an unavoidable background reaction (Liu et al., 2021; Zhao, Fan, et al., 2022; Rodrigues et al., 2021).

For a process in which the target solid is $MgSO_3$, this literature must be read both forward and backward. Highly effective oxidation catalysts are not automatically beneficial; they define the kinetic mechanisms that may need to be minimized in the absorber and precipitation circuit. Conversely, if the site prefers $MgSO_4$, sulfuric-acid integration, or another oxidized product, these catalytic routes become enabling technologies. The critical design decision is therefore product-pathway selection before catalyst selection.

Temperature, ionic strength, and model uncertainty

Temperature changes gas solubility, reaction rates, dissolution of MgO/$Mg(OH)_2$, water evaporation, salt solubility, and crystallization kinetics simultaneously. Ionic strength changes activity coefficients and can shift apparent equilibrium boundaries. The electrolyte-NRTL modeling work is especially relevant because it demonstrates that simplified speciation diagrams are insufficient for design once multiple salts and gases are present (Weiß et al., 2023).

A credible pilot program should therefore use measured liquor composition to update a validated thermodynamic model and compare predicted saturation indices with observed nucleation, deposition, and product phase. This model-data loop is a prerequisite for claiming that precipitation has truly been displaced from the absorber.

Table 3 consolidates the thermodynamic and phase-equilibrium evidence that directly constrains the absorber/crystallizer operating window.

Table 3. *Thermodynamic and Phase-Equilibrium Constraints on the Absorber/Crystallizer Window*

Evidence source	System/condition	Key quantitative or phase result	Design implication	Caution
Neta & Huie (1985).	Aqueous S(IV), near ambient	$pKa_1 \approx 1.86$; $pKa_2 \approx 7.2$	Explains broad bisulfite-dominant intermediate-pH region	Values shift with temperature and activity coefficients
Lowell et al. (1977).	$MgSO_3$ hydrates	Ksp for $MgSO_3 \cdot 6H_2O$ $\sim 5.72 \times 10^{-5}$ at 25 °C; hydrate transition near ~40 °C in the simplified system	First saturation/hydrate benchmark for absorber and crystallizer	Real recycle contains sulfate, Ca, Cl, Na and metals that shift phase boundaries
Lowell et al. (1977).	Precipitation kinetics	Hexahydrate formation: tens of minutes; transformation toward trihydrate: hundreds to thousands of minutes	Residence time and seed phase can select product form	Historical laboratory chemistry; scale-up requires continuous tests
Meng et al. (2018).	Ca^{2+}/Mg^{2+}–SO_3^{2-}/SO_4^{2-}–H_2O at 298.15 K	Five crystallization fields, including $MgSO_3 \cdot 6H_2O$ and $MgSO_4 \cdot 7H_2O$	Calcium and sulfate can create competing solids even when $MgSO_3$ is targeted	Single-temperature equilibrium
Weiß & Harasek (2021); Weiß et al. (2021)	MgO–CaO–SO_2–H_2O–O_2	Measured salt-solubility data and process simulation used to minimize precipitation	Supports saturation-index control rather than pH-only control	Model validity depends on electrolyte parameterization
Weiß et al. (2023).	MgO–CaO–CO_2–SO_2–H_2O–O_2, eNRTL	Non-ideal electrolyte model explicitly includes multi-gas/multi-salt interactions	Required for realistic recycle prediction	Needs plant-liquor validation and impurity extensions

Note. Author synthesis from foundational hydrate/acid–base data and the modern electrolyte-modeling studies listed. Numerical values are orientation points, not universal design constants.

Table 3 replaces a pH-only operating philosophy with a phase-aware one. The absorber must be controlled against undersaturation and S(IV) speciation, while the external crystallizer must be controlled against deliberate supersaturation, hydrate selection, seed inventory, residence time, and separability of the recovered solids.

Magnesium Bisulfite Scrubbing with External Sulfite Recovery

Absorption stage: deliberately low solids

The proposed absorption stage circulates a magnesium-containing liquor under conditions that favorthe formation of dissolved bisulfite and rapid SO_2 uptake. The absorber is neither the primary MgO dissolution tank nor the primary crystallizer. This distinction allows nozzle and contactor design to focus on gas-liquid transfer, droplet residence time, pressure drop, mist control, and corrosion. The concept is consistent with simulation and optimization literature indicating that absorber performance is strongly influenced by the liquid-to-gas ratio, geometry, and operating conditions (Liu et al., 2025; Zhao et al., 2021; Wilailak et al., 2021). It is also consistent with the thermodynamic objective identified by Weiß et al. of minimizing precipitation in the absorber through the selection of operating conditions (Weiß et al., 2021).

A low-solids absorber would still require a controlled dissolved-magnesium inventory, make-up water, bleed, and impurity management. The target is not maximum bisulfite concentration at any cost; excessive dissolved salt raises density, viscosity, ionic strength, corrosion risk, and mist carryover. The operational optimum will therefore be defined

by a window in which gas absorption is fast, the liquor remains sufficiently undersaturated with respect to troublesome solids, and recycle properties remain compatible with pumps and nozzles.

External neutralization, precipitation, and solids separation

The rich bisulfite liquor is transferred to an external reactor where MgO or $Mg(OH)_2$ addition raises alkalinity and converts a selected fraction of dissolved bisulfite toward sulfite. By imposing supersaturation in a well-mixed vessel with controlled residence time, temperature, and seed inventory, nucleation and crystal growth can be shifted away from absorber internals. The target solid must be specified by phase and hydrate rather than generically as $MgSO_3$: depending on temperature, electrolyte composition, and kinetic history, $MgSO_3 \cdot 6H_2O$ and $MgSO_3 \cdot 3H_2O$ can differ in stability and growth behavior (Lowell et al., 1977; Meng et al., 2018). Product specification should therefore include phase identity, particle-size distribution, morphology, settling rate, filtration resistance, and mother-liquor entrainment. The external reactor can then be followed by thickening, filtration, centrifugation, or another solid–liquid separation step. Existing magnesium-sulfite by-product work shows that $MgSO_3$-bearing solids can be separated and treated as recoverable material rather than only as waste (Liao et al., 2023; Du et al., 2022; Jeoung et al., 2026; Khatsevych et al., 2024).

Figure 4 is inserted here as the reference reaction-zone and steady-state recycle architecture used throughout the remainder of the review.

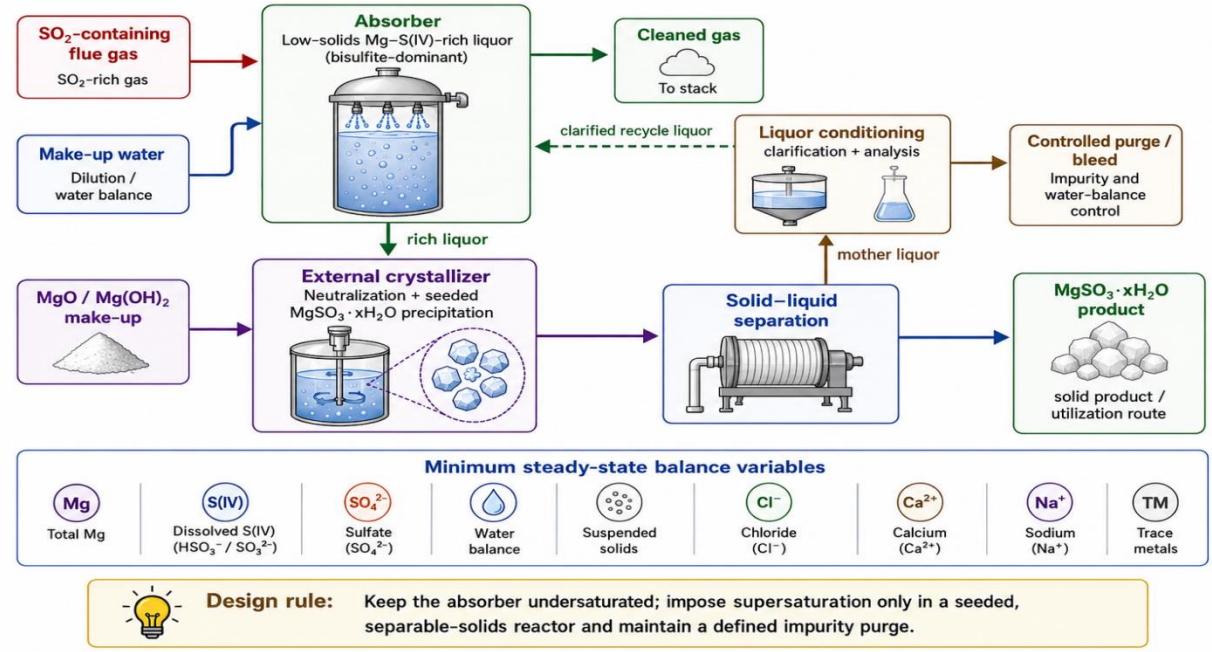

Figure 4. *Proposed Magnesium-Bisulfite Absorption Loop with External Controlled $MgSO_3$ Precipitation*

Note. Author synthesis adapted from historical/regenerative MgO-FGD architecture (U.S. Environmental Protection Agency, 1981; Tian et al., 2021), precipitation-avoidance modeling (Weiß et al., 2021), and the phase/kinetic evidence summarized in Table 3.

Figure 4 shows why the configuration is better described as a rearrangement of reaction zones than as a new absorbent. The low-solids absorber and external crystallizer exchange liquor but can operate at different pH values, residence times, mixing intensities, and saturation states. A credible steady-state balance must track total Mg, dissolved S(IV), sulfate, water, suspended solids, chloride, calcium, sodium, and trace metals across rich liquor, product cake, clarified recycle, purge, and make-up streams. The purge is essential: without a defined bleed, non-precipitating sulfate and impurity species can accumulate until activity coefficients, corrosion, mist loading, or unintended salt precipitation invalidate the low-solids premise.

Regeneration and alternative sulfur products

External treatment does not have to end in $MgSO_3$ recovery. Historical MgO-FGD practice already coupled sulfite solids separation with thermal regeneration and sulfur recovery (Koehler, 1977; U.S. Environmental Protection Agency, 1981). Industrial-demonstration work later examined sulfur recovery from magnesia-WFGD by-products and showed that calciner gas composition is strongly constrained by excess air and regeneration conditions (Yan et al., 2014). More recent work demonstrated simultaneous magnesia regeneration and SO_2 generation, including sulfur-assisted regeneration that reduced the required temperature and produced concentrated SO_2 (Tian et al., 2021). Sodium-based Wellman–Lord-type regeneration similarly illustrates the value of reversible absorption when a site can use or convert recovered SO_2 (Sun et al., 2021). Magnesium-sulfite disproportionation and electrochemically mediated SO_2 treatment further expand the possible product slate (Roshan et al., 2026; Jeong et al.,

2024). The proposed flowsheet should therefore be viewed as a platform: externalization of rich-liquor treatment makes multiple downstream recovery routes accessible without redesigning the gas absorber.

Integration with metallurgical off-gases

Metallurgical integration is attractive because existing smelters already manage sulfuric-acid production, fluctuating sulfur loads, high-temperature gas cooling, dust, and impurity removal. Copper-industry reviews and acid-plant dynamic modeling show that full-process sulfur management increasingly depends on coordination between furnace operation, gas-cleaning capacity, and acid-plant response (Dijkstra et al., 2025; Li et al., 2026; Schmidt & Shang, 2026). PGM and electric-furnace smelting studies likewise show that sulfur-abatement solutions must tolerate transient or dilute streams (Hundermark et al., 2026; Tisdale et al., 2021; Ndlovu et al., 2023). A magnesium-bisulfite polishing or side-stream unit could therefore be most valuable where acid-plant feed requirements leave a residual gas fraction that is too dilute, too variable, or too intermittent for direct acid conversion.

Why Separate Absorption and Precipitation?

Hydrodynamic advantage: remove solids duty from the gas contactor

The strongest engineering argument for separation is hydrodynamic. A gas absorber benefits from uniform liquid distribution, stable nozzle performance, predictable droplet size, low pressure drop, and high interfacial renewal. A crystallizer benefits from controlled supersaturation, sufficient residence time, seed retention, and solids growth. Combining these functions forces a compromise. The scale-control literature demonstrates how precipitation on surfaces and suspended solids amplify one another in wet scrubbers (Fungene et al., 2023). Thermodynamic optimization aimed at minimizing precipitation in SO_2 absorbers aligns with the same objective from a different discipline (Weiß et al., 2021).

The separation advantage remains conditional on saturation control. If the absorber pH is raised too far, water evaporates excessively, or if recycle impurities shift activity coefficients, $MgSO_3$ or other salts can precipitate in the scrubber, and the process reverts to the coupled behavior it was designed to avoid. Consequently, saturation index, conductivity/density, sulfate fraction, and solids carryover should be treated as primary control variables alongside pH and outlet SO_2.

Mass-transfer advantage and mist control

Low-solids circulation can reduce nozzle wear and allow smaller droplet orifices and higher effective interfacial area, although the actual design must balance entrainment and pressure drop. Three-dimensional WFGD studies show that transfer performance is sensitive to the hydrodynamic field and not simply to reagent stoichiometry (Liu et al., 2025). Simulations similarly demonstrate that operating variables interact strongly (Zhao et al., 2021). The proposed benefit is therefore indirect: removing suspended product solids can enlarge the feasible hydrodynamic operating envelope of the absorber.

Figure 5 is inserted here to relate this hydrodynamic argument to reactive-film behavior.

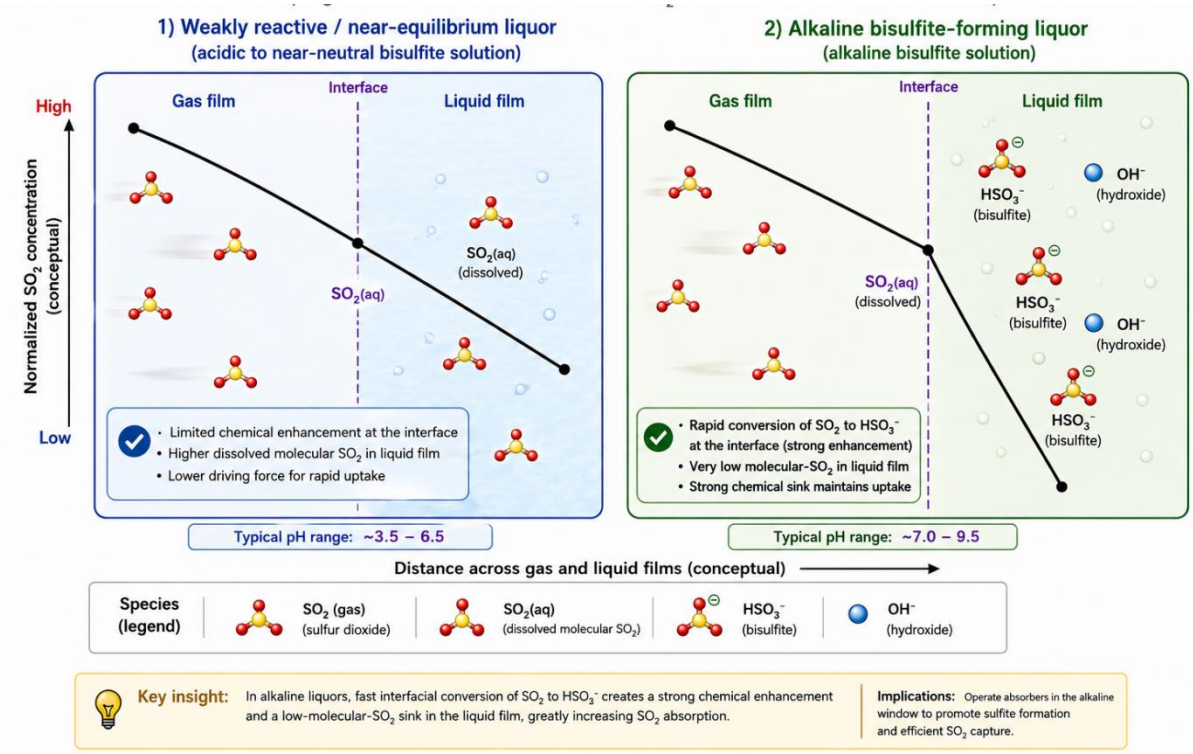

Figure 5. *Conceptual Two-Film Interpretation of SO_2 Absorption With and Without Strong Liquid-Phase Chemical Enhancement*

Note. Author synthesis adapted from the mass-transfer analyses of Zhao et al. (2021), Liu et al. (2025), and Wilailak et al. (2021). Concentration profiles are conceptual and illustrate chemical enhancement rather than fitted plant data.

As illustrated in Figure 5, the purpose of maintaining a bisulfite-forming alkaline sink is to prevent dissolved molecular SO_2 from accumulating near the interface. The chemical enhancement is useful only while the liquid remains hydraulically manageable and thermodynamically stable. This reinforces a general principle: mass transfer, speciation, and precipitation must be optimized together rather than sequentially.

Independent optimization and advanced control

Once the absorber and solids reactor are separated, their control objectives can also be separated. The absorber can be controlled on outlet SO_2, pH, L/G, density/conductivity, and perhaps calculated saturation state. The external reactor can be controlled on supersaturation, seed inventory, residence time, product particle size, and mother-liquor composition. Multi-objective optimization of FGD and hybrid modeling of oxidation processes demonstrate the value of data-driven or surrogate-assisted approaches when competing objectives cannot be collapsed into one set point (Dong et al., 2021; Zhao, Fan, et al., 2022). Recent tail-gas prediction work further indicates that dynamic soft sensors can support earlier detection of off-spec sulfur emissions (Zeng et al., 2026).

Process analytical technology can strengthen this architecture. Raman-based process intensification in chemical-recovery service is not a direct FGD analogue, but it demonstrates the broader feasibility of using in situ spectroscopy to track reactive-liquor chemistry and improve closed-loop recovery (Eisenköck et al., 2025). For magnesium-bisulfite service, analogous measurements of S(IV)/sulfate, dissolved magnesium, solids, and impurity species would reduce dependence on pH as a surrogate for the entire chemistry.

Failure modes created by the new architecture

Decoupling also creates new failure modes. A precipitation reactor can become seed-starved and generate fines; excessive neutralization can create rapid uncontrolled nucleation; recycle clarification can be incomplete; product solids can re-dissolve if the mother liquor is returned under different temperature or pH; and oxygen ingress can progressively convert the S(IV) inventory to sulfate. Reagent suspension stability and $Mg(OH)_2$ microstructure become important because inconsistent alkalinity release can destabilize both vessels (Zhao et al., 2025; von Hoessle et al., 2021). These risks are manageable in principle, but they must be demonstrated under continuous recycle before the concept can be ranked against an industrial calcium benchmark.

Comparative Assessment and Process-Intensification Opportunities

Benchmark comparison: calcium versus magnesium-bisulfite circulation

Table 4 compares the two process philosophies on criteria that matter at plant scale. The ranking remains intentionally qualitative because the literature does not provide a common head-to-head dataset under identical conditions for gas, water, reagents, impurities, and products.

Table 4. *Critical Comparison of Conventional Calcium WFGD and the Proposed Magnesium-Bisulfite/External-Precipitation Configuration*

Criterion	Calcium WFGD	Mg-bisulfite + external precipitation	Critical interpretation
SO_2 capture chemistry	Strong neutralization in circulating slurry	Reactive absorption in dissolved Mg/S(IV) liquor	Both can be effective; mass transfer and operating window govern plant performance
Solids in absorber	Intrinsic and often high	Designed to be low	Potential Mg advantage only if saturation control succeeds
Scaling/plugging	Managed but persistent risk	Potentially lower in absorber	Risk shifts to dedicated precipitation equipment rather than disappearing
Reagent cost/supply	Usually favorable and globally standardized	Often higher and more quality-sensitive	Site-specific delivered cost and MgO reactivity can dominate
Reagent-production burden	Established limestone/lime supply chain	Calcination/hydration route can carry higher embodied energy	Environmental benefit cannot be inferred from absorber operation alone
Dissolved-salt / corrosion burden	Slurry chemistry well characterized	Higher dissolved Mg/S(IV)/SO_4^{2-} inventory may increase ionic strength, density and corrosion	Materials selection and liquor concentration become primary design variables
Sulfate/impurity accumulation	Managed through purge and gypsum circuit	Can progressively alter saturation, product purity and recycle chemistry	Defined bleed and water balance are mandatory
Mist / dissolved carryover	Well-known controls and wash practice	Lower solids may help, but dissolved Mg salts can still be entrained	Mist-eliminator duty does not disappear
By-product handling	Established gypsum route	$MgSO_3$/$MgSO_4$/SO_2 regeneration options	Greater flexibility but less standardized markets/infrastructure
CAPEX / process complexity	Mature integrated slurry loop	Additional conditioning, crystallization, solid–liquid separation and instrumentation	Extra unit operations may purchase lower absorber burden
Reagent loss/purge	Well characterized	Potential Mg loss in product cake, purge and entrainment	Recycle efficiency must be demonstrated
Technology readiness	Commercial benchmark	Components mature; integrated low-solids/external-precipitation architecture at bench-to-pilot level	External controlled $MgSO_3$ crystallization and recycle stability are the least mature elements

Note. Author synthesis based on Kumar and Jana (2022), Xie et al. (2024), Hanif et al. (2020), Stanienda-Pilecki (2021), Tang et al. (2024), historical MgO-FGD operation (Koehler, 1977; U.S. Environmental Protection Agency, 1981), and the thermodynamic/kinetic evidence summarized in Tables 2–3.

Table 4 therefore supports a niche, site-selective interpretation rather than universal substitution. Sites with inexpensive limestone, reliable gypsum disposal or markets, stable gas loads, and mature maintenance practice may have little incentive to change. Sites where scaling drives availability loss, where sulfur products carry higher value, or where water/solids constraints are severe may assign greater value to decoupling. The relevant comparison is annualized total cost and availability per tonne of sulfur captured, not reagent price alone.

Reviews of wet/dry FGD and more recent technology surveys support this site-specific framing (Kumar & Jana, 2022; Xie et al., 2024; Hu et al., 2026; Zheng et al., 2025). Regenerative-FGD reviews also show that a technically more complex process can be justified when sulfur recovery or reagent recycle creates sufficient value (Hanif et al., 2020). Magnesium-enhanced lime and magnesium-bearing limestone studies further illustrate that calcium and magnesium chemistry need not be treated as mutually exclusive categories (Stanienda-Pilecki, 2021; Tang et al., 2024). Hybridization may be more practical than wholesale substitution at some sites.

External crystallization and seeded precipitation

The first intensification opportunity is to design the external solids reactor as a true crystallizer rather than a neutralization tank. Seeded crystallization can reduce uncontrolled primary nucleation, increase product particle size, improve thickening/filtration, and stabilize supersaturation. Foundational hydrate kinetics show that $MgSO_3 \cdot 6H_2O$ can nucleate rapidly while conversion toward $MgSO_3 \cdot 3H_2O$ may occur on much longer time scales, so seed identity and residence time can change the recovered phase (Lowell et al., 1977). The available modern magnesium-FGD literature remains richer on oxidation than on controlled $MgSO_3$ crystallization. Thermodynamic precipitation studies (Weiß et al., 2021; Weiß & Harasek, 2021), mixed-electrolyte phase equilibrium (Meng et al., 2018), and downstream $MgSO_3$ separation (Liao et al., 2023) define the minimum research program: map supersaturation, establish nucleation and growth kinetics, quantify hydrate/morphology selection, and demonstrate separable solids under continuous recycle.

Oxidation control: accelerate, suppress, or spatially confine

The unusually large catalyst literature for $MgSO_3$ oxidation creates a process-design opportunity. Cobalt-based MOFs, Co@NC, $Co(OH)_2/TiO_2$, Mn@ZIF-derived materials, supported cobalt, bimetallic membranes, and other catalysts have been developed to accelerate oxidation and, in some cases, couple it with heavy-metal capture (Li et al., 2020; J. Feng et al., 2024; L. Wang et al., 2020; Xing et al., 2020; Zeng et al., 2025; L. Feng et al., 2024; Geng et al., 2023; Li et al., 2025; Qi et al., 2021; Qi et al., 2023). Rather than adding such catalysts indiscriminately, an intensified plant can spatially confine oxidation to a dedicated reactor. This allows the absorber to preserve S(IV) when $MgSO_3$ is desired, or allows rapid sulfate production when $MgSO_4$ or oxidized by-products are preferred.

Multi-functional materials expand this idea by coupling sulfite oxidation with uptake of arsenic, mercury, selenium, or lead (Liang et al., 2022; Qi et al., 2026; Y. Wang et al., 2020; Xing et al., 2022; Yang et al., 2026; Zhang et al., 2021). These materials are promising for polishing or by-product purification, but they also raise questions about catalyst lifetime, metal leaching, separation, and regeneration. The critical review concludes that catalytic oxidation is a modular intensification option, not part of the minimum viable magnesium-bisulfite flowsheet.

Membranes, electrochemical treatment, and advanced separation

Hydrophobic catalytic membranes have been studied for sulfite oxidation (L. Feng et al., 2024; Meng et al., 2023), while electrochemically mediated SO_2 treatment has been coupled with CO_2 purification and hydrogen production (Jeong et al., 2024; Mousavi et al., 2023). These routes could be integrated downstream of a low-solids absorber more readily than into a high-solids slurry because membrane and electrochemical devices generally prefer controlled solids and impurity loads. This is a second-order benefit of decoupling: once the gas contactor is no longer the location where all sulfur chemistry must be completed, specialized downstream units become technically more accessible.

Product valorization as a design variable

By-product valorization should be selected before the final flowsheet is fixed. Magnesium-FGD residues have been investigated for magnesium metal production, magnesium oxysulfate cement, potassium-magnesium fertilizer, hydrothermal recovery and reuse, chromium removal, and wastewater treatment (Jeoung et al., 2026; Du et al., 2022; Khatsevych et al., 2024; Liu et al., 2022; Fang et al., 2026; T. Zhang et al., 2025; Pang et al., 2024; Pereira, 2025; Pereira et al, 2025; Ren et al., 2021). Oxidized products can also support sulfur recovery and the capture of multiple pollutants (Qi et al., 2026). These examples do not prove universal marketability, but they demonstrate that the solid/liquid outputs of magnesium scrubbing can be treated as process intermediates. The external reactor is therefore the logical point at which to tailor the crystal phase, impurity content, oxidation state, and particle size toward a selected downstream use.

Techno-Economic Assessment Framework

Cost architecture rather than reagent-price comparison

Because the reviewed literature does not provide a common plant-scale cost basis for the proposed architecture, this section is an assessment framework rather than a completed techno-economic analysis. A credible comparison must include absorber, pumps, nozzles, conditioning and crystallization tanks, solids separation, reagent preparation, purge/water treatment, mist elimination, corrosion allowance, instrumentation, maintenance, cleaning, waste/by-product handling, energy, and availability. Eco-efficient FGD optimization studies demonstrate the need for multi-objective framing (Dong et al., 2021). Magnesium reagent may carry a higher unit cost and embodied production burden than limestone, while a genuinely low-solids absorber could reduce slurry circulation duty, erosion, cleaning frequency, and blockage. Whether avoided operability costs compensate for extra reagent and equipment is site-specific.

Heat and water integration can materially change the economics. WFGD dehumidification and heat-recovery concepts (Chen et al., 2020), slurry-waste-heat recovery (Zhang et al., 2022), and low-grade heat recovery around sulfuric-acid plants (McLean et al., 2022) show that sulfur control should be evaluated within the site's energy and water network. Magnesium-FGD wastewater concentration studies likewise demonstrate that waste-heat utilization can reduce the cost of managing concentrated liquid streams (Yan & Shi, 2020).

Avoided-operability burden as an economic variable

The proposed process is economically attractive only when the value of avoided absorber burden is quantified. Relevant terms include reduced nozzle replacement, reduced pump wear, reduced wash-water consumption, fewer cleaning outages, lower mist-eliminator fouling, and higher gas-treatment availability. These benefits are often missing from reagent-centric comparisons because they appear in maintenance budgets rather than process-consumables budgets. Conversely, additional crystallizer agitation, solids separation, instrumentation, and magnesium make-up add capital and operating costs. A full comparison should therefore be based on annualized total cost at equal sulfur-removal compliance and equal plant availability.

Figure 6 is inserted here as a qualitative site-selection matrix rather than a calculated economic break-even curve.

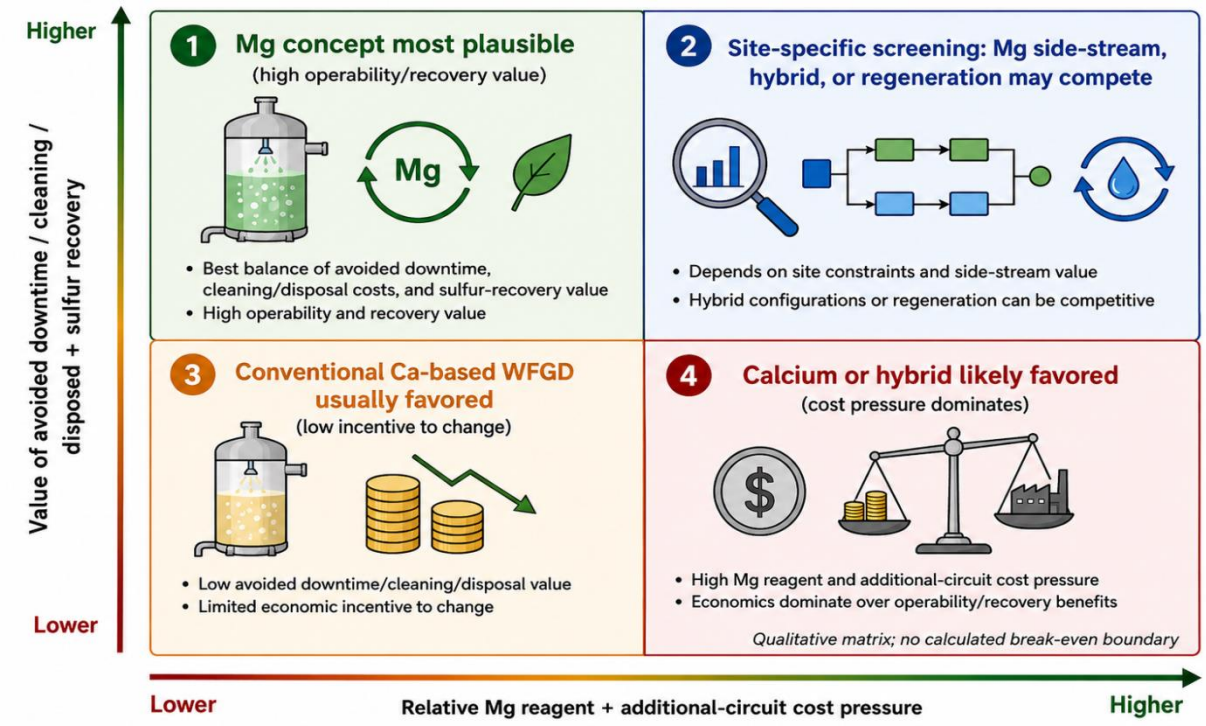

Figure 6. *Qualitative Site-Selection Matrix for Magnesium-Bisulfite Circulation Versus Calcium WFGD*

Note. Author synthesis. The matrix is qualitative and intentionally contains no calculated indifference boundary. Its logic is informed by multi-objective FGD optimization (Dong et al., 2021), heat-recovery studies (Chen et al., 2020; McLean et al., 2022), magnesium-FGD wastewater economics (Yan & Shi, 2020), and the balanced cost factors summarized in Table 4.

Figure 6 deliberately avoids a numerical indifference boundary. When delivered Mg reagent/circuit cost pressure is high, and the value of avoided downtime, cleaning, disposal, or sulfur recovery is low, conventional calcium WFGD is the natural benchmark. The magnesium concept becomes more credible as operability losses and recoverable-product value

increase, particularly where a side-stream or polishing duty limits total magnesium consumption. Intermediate cases favor either hybridization or a site-specific screening study over a universal technology ranking.

By-product revenue and integration credit

Potential credits include regenerated SO_2, magnesium compounds, fertilizer products, cementitious materials, magnesium metal feed, and environmental service value from waste utilization (Tian et al., 2021; Jeoung et al., 2026; Khatsevych et al., 2024; Du et al., 2022; Liu et al., 2022). Calcium FGD gypsum itself can also be valorized, including mineral-carbonation applications (Córdoba & Rojas, 2024); therefore, magnesium should not be assigned circular-economy credit while calcium is treated as pure waste. A fair comparison assigns market value, purification cost, transport, and disposal risk to both routes.

Technology Readiness and Scale-Up

What is already industrially mature

Limestone/lime WFGD, magnesium-enhanced lime, acid-plant sulfur capture, dry gas cleaning for metallurgical SO_2 service, and several regenerative sulfur processes have industrial precedent (Scherman Johansson, 2025; Strong et al., 2025; Weber et al., 2020; Sun et al., 2021). Magnesium-based absorption and regeneration also have a substantial technical basis, including explicit magnesia regeneration/SO_2 Generation studies (Tian et al., 2021). The uncertainty is narrower: continuous industrial operation of a deliberately low-solids magnesium-bisulfite absorber coupled to a dedicated external $MgSO_3$ precipitation step is not established by the supplied evidence base.

Indicative TRL of the proposed configuration

Figure 7 is inserted here to distinguish mature component technologies from the less mature integrated configuration.

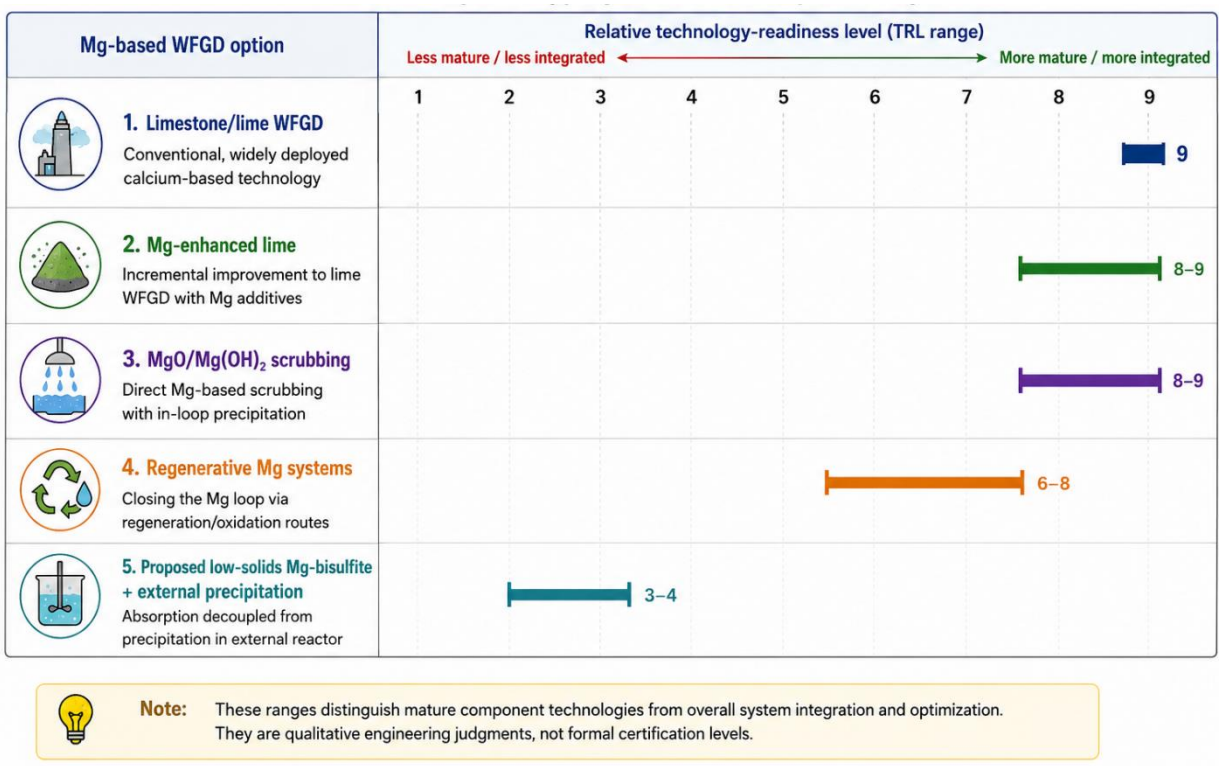

Figure 7. *Indicative Technology-Readiness Ranges for Magnesium-Bisulfite/External-Precipitation FGD*

Note. Author synthesis based on historical and modern industrial sulfur-control evidence. Ranges are qualitative engineering judgments mapped to conventional TRL categories; they are not formal technology certification.

As Figure 7 indicates, most component technologies are individually mature, including absorbers, $MgO/Mg(OH)_2$ handling, neutralization vessels, crystallizers, thickeners/filters, and gas analyzers. Historical full-scale MgO-FGD operation confirms that magnesium scrubbing and regeneration are not intrinsically low-TRL technologies (Koehler, 1977; U.S. Environmental Protection Agency, 1981). The lower readiness lies in the specific integration rule proposed here: maintaining a deliberately low-solids bisulfite absorber while externally forcing controlled $MgSO_3$ precipitation and preserving long-duration recycle stability. Scale-up, therefore, requires validation of the coupled operating envelope rather than inventing each unit operation.

The scale-up sequence should therefore shift from bench-scale equilibrium and crystallization kinetics to a closed, recirculating pilot before any pre-commercial demonstration. Pilot tests must include realistic gas transients, oxygen variation, water evaporation, particulate carryover, acid mist/halides where relevant, and progressive impurity accumulation. Industrial smelter experience shows that gas-

treatment systems must withstand disturbances rather than only steady-state design conditions (Hundermark et al., 2026; Schmidt & Shang, 2026; Tisdale et al., 2021).

Scale-up should be governed by explicit decision gates: validated phase prediction, controllable external crystallization, stable closed-loop recycle, dynamic-gas compliance without absorber precipitation, and finally pre-commercial proof of availability, product quality, maintenance burden, and lifecycle cost.

Continuous recycle is a gate rather than an afterthought. Many laboratory studies demonstrate strong instantaneous chemistry, whereas industrial FGD failures are often driven by accumulation, deposition, transient response, or maintenance issues. Technology readiness should therefore be assigned only after time-dependent behavior is demonstrated.

Environmental Performance and Circularity

Water, effluent, and solids generation

A low-solids absorber may reduce internal solids circulation but does not eliminate water or residuals. Evaporation concentrates chloride, sulfate, calcium, sodium, and trace metals; a bleed stream will usually be required. Water/heat recovery and closed-loop strategies can reduce freshwater demand but increase dissolved salt concentration and therefore must be coordinated with thermodynamic saturation control (Chen et al., 2020; Lee et al., 2023; Zhang et al., 2022). The environmental comparison should report water withdrawal, wastewater volume and composition, total solids generated, hazardous and trace-element partitioning, and product usability.

From waste to product: credible and non-credible circularity claims

The magnesium-FGD literature contains multiple examples of residue utilization: magnesium oxysulfate cement (Du et al., 2022), Mg metal production from sludge cake (Jeoung et al., 2026), potassium-magnesium fertilizer (Khatsevych et al., 2024), hydrothermal recovery/reuse of oxidized products (Liu et al., 2022), Cr(VI) removal (Fang et al., 2026), and wastewater decoloration (T. Zhang et al., 2025). These studies establish technical pathways but not necessarily markets at the scale of a large smelter or power plant. Circularity claims should therefore distinguish laboratory reactivity from bankable offtake. Product purity, logistics, competing materials, and regulatory acceptance determine whether a by-product is a revenue stream or simply a differently named waste.

The same discipline must be applied to calcium gypsum, which can have legitimate uses or carbon sequestration pathways (Córdoba & Rojas, 2024). A comparative life-cycle assessment should credit both routes for real substitution effects and debit both routes for reagent production, energy, water, transport, and residual disposal. Sulfuric acid plant heat-recovery studies show how integration credits can alter environmental performance even when the core sulfur-conversion chemistry remains unchanged (McLean et al., 2022).

Multi-pollutant capture and metallurgical circularity

Magnesium-FGD by-products and catalytic media can capture or immobilize trace metals during sulfur processing (Liang et al., 2022; Qi et al., 2026; Y. Wang et al., 2020; Xing et al., 2022; Yang et al., 2026; Zhang et al., 2021). Metallurgical sorbents based on copper slag, tailings, manganese carbonate, or calcine oxides likewise demonstrate the possibility of combining SO_2 control with extraction or waste utilization (Bao et al., 2021; Tao et al., 2022; Tang et al., 2023; Weng et al., 2023). These strategies are especially relevant for smelters because the gas-cleaning train is already connected to metal-bearing dust and liquid effluent circuits. However, co-capture can contaminate a magnesium sulfate product and reduce its value for reuse. The environmental optimum may therefore require removing impurities before the bisulfite loop rather than maximizing co-capture within it.

Research Gaps, and a Validation Agenda

Thermodynamic databases for real recycle liquors

The first research gap is the lack of a validated electrolyte database for $Mg–SO_2–O_2–H_2O$ systems that includes the impurities expected in industrial recycle. Existing solubility and eNRTL studies provide an essential foundation (Weiß et al., 2021; Weiß et al., 2023; Weiß & Harasek, 2021), and mixed magnesium-sodium thermodynamic work extends the chemical space (Zhong et al., 2026). What is still needed is systematic validation against representative chloride, sulfate, calcium, sodium, arsenic, heavy-metal, and particulate-derived species over the absorber/crystallizer temperature range. The design target should be a reliable saturation-index calculation that predicts both desired $MgSO_3$ precipitation and undesired scale phases.

Coupled dissolution and crystallization kinetics

The second gap is kinetic. MgO dissolution studies (Ma et al., 2024), particle-size effects (Zhao & Zou, 2021), hydration/microstructure work (Tang et al., 2020; Zhu et al., 2026), and hydroxide interfacial studies (von Hoessle et al., 2021) describe how alkalinity becomes available. Less developed in the supplied corpus is the controlled nucleation and crystal growth of $MgSO_3$ under continuous recycling. The external-reactor concept cannot be optimized from equilibrium alone because industrial separability depends on particle-size distribution, agglomeration, morphology, and settling/filtration behavior.

Oxidation selectivity and product-pathway control

The third gap is not a lack of knowledge of oxidation but a lack of process-selective use of that knowledge. The catalyst literature is extensive (Fang et al., 2021; J. Feng et al., 2024; L. Feng et al., 2024; Geng et al., 2023; Li et al., 2020; Li et al., 2025; Qi et al., 2021; Qi et al., 2023; L. Wang et al., 2020; Y. Wang et al., 2020; Xing et al., 2020; Zeng et al., 2025) and process optimization has been studied (Liu et al., 2021; Zhao, Fan, et al., 2022). The missing question for $MgSO_3$ recovery is how to sufficiently suppress oxidation in the absorber and precipitation circuit without creating unacceptable oxygen-control or corrosion requirements, or, alternatively, how to confine accelerated oxidation to a dedicated downstream step. This should be studied with mass-transfer-based oxygen balances rather than catalyst screening alone.

Pilot demonstration under metallurgical transients

The fourth gap is integrated pilot evidence under dynamic gas loads. Smelter technology studies (Strong et al., 2025; Hundermark et al., 2026; Tisdale et al., 2021; Weber et al., 2020) and acid-plant dynamics (Schmidt & Shang, 2026) show that real sulfur-control systems experience rapidly changing flow and composition. A pilot should therefore be challenged with load ramps, high- and low-SO_2 conditions, oxygen variations, dust breakthroughs, water-balance changes, and controlled impurity spikes. Tail-gas prediction and advanced control methods (Zeng et al., 2026) can be evaluated at this stage, but only after the physical chemistry is sufficiently understood to prevent a data-driven controller from masking an unstable process.

Integration with sulfur recovery, energy, and product systems

The fifth gap is systems integration. Regeneration to SO_2 (Tian et al., 2021), magnesium-sulfite disproportionation (Roshan et al., 2026), Wellman-Lord-type regeneration (Sun et al., 2021), electrochemical treatment (Jeong et al., 2024), heat recovery (McLean et al., 2022), and water/heat recovery (Chen et al., 2020) create multiple downstream options. The research program should compare them using a common functional basis: tonne of sulfur captured at the required emission limit, including energy, water, reagent make-up, product value, and availability.

The research tasks are coupled. A thermodynamic model without crystallization kinetics cannot size the external reactor; crystallization kinetics without pilot hydrodynamics cannot guarantee absorber cleanliness; pilot hydrodynamics without impurity and product analysis cannot establish circularity; and all of these without a systems-level cost model cannot establish a business case.

Table 5 consolidates the research questions into measurable outputs suitable for a staged development program.

Table 5. *Priority Research Questions and Measurable Outputs*

Priority	Research question	Measurable output	Why it matters
1	What is the absorber precipitation boundary for real liquor?	Validated saturation model and operating map	Protects the low-solids premise
2	How fast does $MgSO_3$ nucleate and grow externally?	Kinetic model, PSD, settling/filtration data	Sizes crystallizer and separator
3	How rapidly does S(IV) oxidize unintentionally?	Oxygen-transfer/oxidation model under realistic impurities	Determines product selectivity and reagent balance
4	Does recycle remain stable for long duration?	Mass balance closure over many cycles	Reveals sulfate/impurity accumulation
5	How does the process behave during gas transients?	Dynamic emission, pH, saturation and mist response	Establishes industrial operability
6	Where is the economic break-even?	Annualized lifecycle cost and availability sensitivity	Defines viable site archetypes

Note. Author synthesis from the evidence and scale-up gaps identified in Sections 3–12.

The agenda in Table 5 is intentionally narrower than a general magnesium-FGD research program. Its purpose is to test the specific causal claim advanced by this review: that moving precipitation outside the absorber creates enough operability and control value to justify the extra process equipment and magnesium cost.

Conclusions

Calcium-based WFGD remains the industrial benchmark because low-cost reagents, proven equipment, and established by-product handling offset the burden of operating a solids-rich slurry loop. The critical comparison developed in this review therefore does not support a universal substitution of calcium by magnesium. It identifies a narrower process-intensification hypothesis: SO_2 can potentially be captured in

a predominantly dissolved magnesium-bisulfite inventory while neutralization and magnesium-sulfite precipitation are transferred to a dedicated external crystallizer.

The principal potential advantage is the creation of independent operating windows for gas–liquid mass transfer and solids formation rather than a fundamentally higher equilibrium removal efficiency. That advantage is conditional. If absorber saturation, water balance, sulfate accumulation, or impurity loading are not controlled, precipitation can migrate back into the gas contactor, eliminating the hydrodynamic benefit. Likewise, sulfite oxidation must be deliberately selected as a product pathway: it may need to be suppressed when $MgSO_3$ recovery is targeted, or accelerated in a separate reactor when $MgSO_4$, regenerated SO_2, or another oxidized sulfur product is preferred.

The largest evidence gap is integrated continuous operation. Thermodynamic plausibility, historical MgO-FGD experience, and strong laboratory chemistry do not establish that the proposed low-solids/external-precipitation architecture can maintain long-duration recycle stability, predictable hydrate and particle-size distributions, impurity tolerance, low mist loading, acceptable materials performance, and dynamic emission control. A credible development program must therefore close equilibrium, crystallization kinetics, hydrodynamics, recycle mass balance, and materials questions together rather than sequentially.

Technology selection should ultimately be based on annualized lifecycle cost and plant availability at equal sulfur-removal compliance, with realistic values assigned to both calcium and magnesium by-products. The most efficient validation path is staged: electrolyte-thermodynamic validation with real liquors, $MgO/Mg(OH)_2$ dissolution and $MgSO_3$ hydrate/crystallization kinetics, closed-loop pilot testing, dynamic metallurgical-gas challenge tests, and finally a long-duration industrial side-stream demonstration.

Declarations

Funding: No external funding was received for this work.

Conflict of interest: The author declares no known competing financial interests or personal relationships that could have appeared to influence the work.

Data availability: No new experimental dataset was generated for this critical review; the evidence base consists of the literature cited in the manuscript.

Author contributions: Antonio Clareti Pereira: Conceptualization, Methodology, Investigation, Data curation, Formal analysis, Visualization, Writing – original draft, Writing – review & editing.

References

1. Bakhshi Ani, A., & Ale Ebrahim, H. (2020). Theoretical and experimental investigation on improvement of magnesium oxide sorbent by acetic acid washing for enhancing flue gas desulfurization performance. *Chemical Papers, 74*(8), 2471–2479. https://doi.org/10.1007/s11696-020-01093-6
2. Bakhshi Ani, A., & Ale Ebrahim, H. (2021a). Comprehensive kinetic study of sulfur dioxide removal by magnesium oxide using TG. *Journal of Thermal Analysis and Calorimetry, 146*(6), 2587–2599. https://doi.org/10.1007/s10973-021-10597-6
3. Bakhshi Ani, A., & Ale Ebrahim, H. (2021b). Modeling and multi-objective optimization of a packed bed reactor for sulfur dioxide removal by magnesium oxide using non-dominated sorting genetic algorithm II. *Chemical and Biochemical Engineering Quarterly, 35*(3), 251–266. https://doi.org/10.15255/CABEQ.2021.1913
4. Bao, J., Xiao, H., Li, K., Wang, C., Song, X., Sun, X., Ning, P., & Luo, Y. (2021). Simultaneous NO_x and SO_2 removal during wet flue gas desulfurization, using copper smelter slag slurry combined with yellow phorphorus. *The Canadian Journal of Chemical Engineering, 99*(6), 1334–1344. https://doi.org/10.1002/cjce.23925
5. Bassioni, G., Farid, R., Mohamed, M., Hammouda, R. M., & Kühn, F. E. (2021). Effect of different parameters on caustic magnesia hydration and magnesium hydroxide rheology: A review. *Materials Advances, 2*(20), 6519–6531. https://doi.org/10.1039/D0MA00887G
6. Cao, W., & Zhang, W. (2020). Experiment and mechanism analysis of desulfurization with a MgO-based desulfurizer fixed bed method. *ACS Omega, 5*(47), 30740–30745. https://doi.org/10.1021/acsomega.0c04967
7. Chen, Z., You, C., Wang, H., & Xie, N. (2020). A novel technical route based on wet flue gas desulfurization process for flue gas dehumidification, water and heat recovery. *Applied Thermal Engineering, 171*, 115102. https://doi.org/10.1016/j.applthermaleng.2020.115102
8. Córdoba, P., & Rojas, S. (2024). Carbon sequestration through mineral carbonation: Using commercial FGD-gypsum from a copper smelter for sustainable waste management and environmental impact mitigation. *Journal of Environmental Chemical Engineering, 12*(2), 112510. https://doi.org/10.1016/j.jece.2024.112510
9. Dijkstra, R., King, M., & Lee, H. (2025). Sulfuric acid production in the copper industry—A review with future insights. In The Metallurgy and Materials Society of CIM, The Society for Mining, Metallurgy & Exploration, & The Minerals, Metals & Materials Society (Eds.), *12th International Copper Conference: Proceedings of the Extraction 2025 Meeting & Exhibition, Volume I* (pp. 39–53). Springer. https://doi.org/10.1007/978-3-032-00102-3_4

10. Dong, Q., Wang, C., Peng, S., Wang, Z., & Liu, C. (2021). A many-objective optimization for an eco-efficient flue gas desulfurization process using a surrogate-assisted evolutionary algorithm. *Sustainability*, *13*(16), 9015. https://doi.org/10.3390/su13169015
11. Du, H., Li, J., Ni, W., Hou, C., & Liu, W. (2022). The hydration mechanism of magnesium oxysulfate cement prepared by magnesium desulfurization byproducts. *Journal of Materials Research and Technology*, *17*, 1211–1220. https://doi.org/10.1016/j.jmrt.2022.01.070
12. Eisenköck, M., Schwaiger, A. K., Ramer, G., Lendl, B., & Wieland, K. (2025). Process intensification of the chemical recovery in the pulp and paper industry using Raman spectroscopy. *Analytical and Bioanalytical Chemistry*, *417*(25), 5637–5649. https://doi.org/10.1007/s00216-025-06015-7
13. Fang, D., Li, X., & Xue, X. (2026). A environment-friendly utilization of flue gas desulfurization residue for removing hexavalent chromium from electroplating wastewater. *Transition Metal Chemistry*, *51*(2), Article 27. https://doi.org/10.1007/s11243-026-00714-5
14. Fang, Z., Xing, L., Liu, Y., Guo, X., Qi, T., Liu, J., & Wang, L. (2021). Ternary heterojunction stabilized photocatalyst of Co-TiO_2/g-C_3N_4 in boosting sulfite oxidation during wet desulfurization. *Applied Surface Science*, *551*, 149478. https://doi.org/10.1016/j.apsusc.2021.149478
15. Feng, J., Geng, N., Wang, F., Wang, F., Ning, P., Ma, L., & Jia, L. (2024). ZIF-67-derived Co@NC as an efficient catalyst for magnesium sulfite oxidation in the flue gas desulfurization process. *Fuel*, *367*, 131433. https://doi.org/10.1016/j.fuel.2024.131433.
16. Feng, L., Liu, J., Wang, S., Zhao, Y., Li, F., Guo, X., & Yuan, J. (2024). Preparation of Fe/Co bimetallic oxide loaded hydrophobic & catalytic bifunctional membrane and its catalytic performance in sulfite oxidation. *Heliyon*, *10*(15), e34789. DOI: 10.1016/j.heliyon.2024.e34789. DOI
17. França, Í. W. L., Cartaxo, S. J. M., Bastos-Neto, M., Gonçalves, L. R. B., & Fernandes, F. A. N. (2020). Effect of additives to improve calcium-based sorbents in semi-dry flue gas desulphurization. *Emission Control Science and Technology*, *6*(1), 105–112. DOI: 10.1007/s40825-020-00156-0. DOI
18. Fungene, T., Ndlovu, S., & Matinde, E. (2023). Scale formation in wet scrubbers and the current state of anti-scaling and softening methods for hard waters: A review. *Separation Science and Technology*, *58*(7), 1331–1346. DOI: 10.1080/01496395.2023.2189051. DOI
19. Geng, N., Wang, F., He, D., Wang, F., Xia, F., Feng, J., Jia, L., Wang, L., & Ning, P. (2023). Novel cobalt-based MOF facilitating reclaiming byproduct in wet magnesia desulfurization with ultrahigh dispersity and catalytic activity. *Fuel*, *341*, 127021. DOI: 10.1016/j.fuel.2022.127021. DOI
20. Ghosh, D., Biswas, D., & Datta, A. (2026). Absorption height in spray tower for wet-limestone process in flue gas desulphurization. *Materials Today: Proceedings*, *126*, 30–35. DOI: 10.1016/j.matpr.2024.02.001. DOI
21. González, M., Martínez, A., & Mercado, F. (2025). Designing gas cleaning plants for E-scrap recycling furnaces. In The Metallurgy and Materials Society of CIM, The Society for Mining, Metallurgy & Exploration, & The Minerals, Metals & Materials Society (Eds.), *12th International Copper Conference: Proceedings of the Extraction 2025 Meeting & Exhibition, Volume I* (pp. 2761–2771). Springer. Página verdadeira do capítulo – Springer Professional
22. Guo, J., Xiong, J., Li, Y., Qinggele, J., & Zhu, T. (2025). Absorption mechanism of SO_3 on various alkaline absorbents in the presence of SO_2. *Journal of Environmental Sciences*, *149*, 268–277. DOI: 10.1016/j.jes.2023.11.013. DOI
23. Hanif, M. A., Ibrahim, N., & Abdul Jalil, A. (2020). Sulfur dioxide removal: An overview of regenerative flue gas desulfurization and factors affecting desulfurization capacity and sorbent regeneration. *Environmental Science and Pollution Research*, *27*(22), 27515–27540. DOI: 10.1007/s11356-020-09191-4. DOI
24. He, X., Fan, X., You, C., Wang, H., & Jin, Y. (2025). Reaction mechanism and efficiency enhancement of dry desulfurization at high temperature of magnesian hydrated lime. *Journal of China Coal Society*, *50*(10), 4840–4851. DOI: 10.13225/j.cnki.jccs.2024.0922. DOI
25. Hu, S., Pan, Y., Chen, W., & Zhang, Y. (2026). Research progress on flue gas SO_2 capture. *Separation Science and Technology*. Advance online publication. DOI: 10.1080/01496395.2026.2651748. DOI
26. Huang, W., Li, S., Wang, H., Cui, P., Xu, H., Cheng, C., Qu, Z., & Yan, N. (2022). Buffer effect of MgO on Na_2SO_3 to stabilize S(IV) for the enhancement in simultaneous absorption of NO_x and SO_2 from non-ferrous smelting gas. *Environmental Science and Pollution Research*, *29*(47), 71721–71730. DOI: 10.1007/s11356-022-20748-3. DOI
27. Hundermark, R., Marsden, G., Snodgrass, R., & van der Merwe, K. (2026). Technology evolution in the Southern African Ni-Cu-Platinum Group Metals (PGM) smelting industry. *Journal of the Southern African Institute of Mining and Metallurgy*, *126*(7). DOI: 10.17159/2411-9717/1048/2026. DOI
28. Jeong, U., Lee, G., Kim, H. J., Kim, K., & Han, J. I. (2024). Electrochemically-mediated treatment of sulfur dioxide and purification of carbon dioxide coupled with hydrogen production. *Separation and*

Purification Technology, 330, 125438. DOI: 10.1016/j.seppur.2023.125438. DOI

29. Jeoung, H.-J., Na, H., Lee, T.-H., Yi, K.-W., & Kang, J. (2026). Investigation of the use of sludge cake from Mg-based FGD process for the eco-friendly Mg metal production process. *Journal of Material Cycles and Waste Management, 28*, 1763–1777. DOI: 10.1007/s10163-026-02485-8. DOI
30. Khatsevych, O., Fedorchenko, S., Kurta, S., Mykytyn, I., & Derzhko, O. (2024). Desulfurization of flue gases of thermal power plants with obtaining potassium-magnesium fertilizer (kalimagnesia). *Environmental Problems, 9*(2), 84–88. DOI: 10.23939/ep2024.02.084. DOI
31. Koehler, G. (1977). *Magnesia scrubbing applied to a coal-fired power plant* (EPA-600/7-77-018). U.S. Environmental Protection Agency, Office of Research and Development, Industrial Environmental Research Laboratory. U.S. EPA – relatório original
32. Kumar, L., & Jana, S. K. (2022). Advances in absorbents and techniques used in wet and dry FGD: A critical review. *Reviews in Chemical Engineering, 38*(7), 843–880. DOI: 10.1515/revce-2020-0029. DOI
33. Lee, I., Chang, T., Chang, C., Truong, V. D. H., & Ward, J. D. (2023). Comparison of open- and closed-loop operating strategies for exhaust gas scrubbing in marine applications: Modeling and sea-trial data. *Proceedings of the Institution of Mechanical Engineers, Part M: Journal of Engineering for the Maritime Environment, 237*(2), 370–384. DOI: 10.1177/14750902221123845. DOI
34. Li, M., Guo, Q., Xing, L., Yang, L., Qi, T., Xu, P., Zhang, S., & Wang, L. (2020). Cobalt-based metal-organic frameworks promoting magnesium sulfite oxidation with ultrahigh catalytic activity and stability. *Journal of Colloid and Interface Science, 559*, 88–95. DOI: 10.1016/j.jcis.2019.10.004. DOI
35. Li, N., Gao, C., Guo, Z., & Zhang, M. (2026). Towards ultra-low sulfur dioxide emissions in copper industry: An integrated analysis based on full-process material-energy-pollution flows. *Process Safety and Environmental Protection, 215*, 109210. DOI: 10.1016/j.psep.2026.109210. DOI
36. Li, Z., Tang, X., Wang, F., Li, K., Lei, S., Ning, P., Ma, X., & Sun, X. (2025). The catalytic mechanism of cobalt-based sites in the oxidation of $MgSO_3$. *Process Safety and Environmental Protection, 194*, 752–760. DOI: 10.1016/j.psep.2024.12.018. DOI
37. Liang, Z., Qi, T., Liu, H., Wang, L., & Li, Q. (2022). Zero-valent bimetallic catalyst/absorbent for simultaneous facilitation of $MgSO_3$ oxidation and arsenic uptake. *Science of the Total Environment, 844*, 157147. DOI: 10.1016/j.scitotenv.2022.157147. DOI.
38. Liao, S., Yang, Y., Li, Y., & Wu, H. (2023). Study on flotation experiment and mechanism of desulfurization by-product magnesium sulfite using dodecylamine. *Inorganic Chemicals Industry, 55*(2), 113–118. https://doi.org/10.19964/j.issn.1006-4990.2022-0143
39. Liu, C., Zhao, Z., Gao, W., Baleta, J., Li, W., Li, Q., Shen, M., Zheng, C., & Gao, X. (2021). Process optimization of S(IV) oxidation in flue gas desulfurization scrubbers. *Process Safety and Environmental Protection, 149*, 610–618. https://doi.org/10.1016/j.psep.2021.03.020
40. Liu, H., Shen, F., Li, Q., Wen, M., Zhang, H., Jiang, L., Zheng, C., Liu, Y., Liu, T., & Chai, L. (2023). Systematic control technologies for gaseous pollutants from non-ferrous metallurgy. *Journal of Environmental Sciences, 123*, 65–82. https://doi.org/10.1016/j.jes.2022.01.035
41. Liu, P., Yang, S., & Wang, H. (2025). Mass transfer behavior and desulfurization characteristics in the three-dimensional wet flue gas desulfurization tower. *Energy, 319*, 134840. https://doi.org/10.1016/j.energy.2025.134840
42. Liu, Y., Shi, P., & Jiang, M. (2022). Hydrothermal recovery and reuse of oxidated by-products in magnesium flue gas desulfurization: Experimental studies and molecular dynamics simulation. *Journal of Environmental Chemical Engineering, 10*(3), 108099. https://doi.org/10.1016/j.jece.2022.108099
43. Lowell, P. S., Meserole, F. B., & Parsons, T. B. (1977). *Precipitation chemistry of magnesium sulfite hydrates in magnesium oxide scrubbing* (EPA-600/7-77-109). U.S. Environmental Protection Agency, Office of Research and Development, Industrial Environmental Research Laboratory. EPA official record
44. Ma, M., Zhao, H., & Hu, P. (2024). Investigation into the dissolution kinetics of different MgO desulfurizers in flue gas desulfurization. *ACS Omega, 9*(11), 12779–12788. https://doi.org/10.1021/acsomega.3c08575
45. McLean, S. H., Chenier, J., Muinonen, S., Moreau, K., Laamanen, C. A., & Scott, J. A. (2022). A case study comparison of a sulphuric acid plant with and without on-site low-grade heat recovery and repurposing. *The International Journal of Life Cycle Assessment, 27*(5), 655–664. https://doi.org/10.1007/s11367-022-02052-x
46. Meng, H., Bi, J., Liu, J., Wang, S., Ji, Z., Zhao, Y., Li, F., Guo, X., & Yuan, J. (2023). MnO_2-functionalized hydrophobic ceramic membrane for sulfite oxidation. *ACS Applied Nano Materials, 6*(8), 6772–6783. https://doi.org/10.1021/acsanm.3c00491
47. Meng, X., Wu, X., & Yuan, J. (2018). Solid–liquid equilibrium of the quaternary system Ca^{2+}, Mg^{2+}//SO_3^{2-}, SO_4^{2-}–H_2O at 298.15 K. *Journal of Chemical & Engineering Data, 63*(12), 4339–4349. https://doi.org/10.1021/acs.jced.8b00385
48. Mousavi, S. E., Pahlavanzadeh, H., Khalighi, R., Khani, M., Ale Ebrahim, H., Abbasizadeh, S., & Mozaffari, A. (2023). Reduction of SO_2 to elemental sulfur in flue gas using copper-alumina catalysts.

Journal of Nanotechnology, 2023, Article 3723612. https://doi.org/10.1155/2023/3723612

49. Ndlovu, M., Marsden, G., Bezuidenhout, J., Hundermark, R., & Erasmus, G. (2023). SO_2 abatement at the Polokwane Smelter—The project and the process. In *8th Sulphur and Sulphuric Acid 2023 Conference Proceedings* (pp. 1–14). Southern African Institute of Mining and Metallurgy. SAIMM conference record
50. Neta, P., & Huie, R. E. (1985). Free-radical chemistry of sulfite. *Environmental Health Perspectives, 64*, 209–217. https://doi.org/10.1289/ehp.8564209
51. Pang, Y., Zhen, F., Wang, D., Luo, Z., Huang, J., & Zhang, Y. (2024). Effects of biochar combined with MgO desulfurization waste residue on nitrogen conversion and odor emission in chicken manure composting. *Environmental Technology, 45*(23), 4779–4790. https://doi.org/10.1080/09593330.2023.2283086
52. Papadopoulos, C., Kourtelesis, M., Moschovi, A. M., Sakkas, K. M., & Yakoumis, I. (2022). Selected techniques for cutting SOx emissions in maritime industry. *Technologies, 10*(5), 99. https://doi.org/10.3390/technologies10050099
53. Pereira, A. C., & Fonseca, R. B. da C. (2025). Synthesis of reactive MgO from hydrated magnesium sulfate via carbothermic reduction. *Revista DELOS, 18*(69), e6030. https://doi.org/10.55905/rdelosv18.n69-145
54. Pereira, A. C. (2025). Reactive magnesia from magnesium sulfate hydrate: A circular route for acid neutralization systems. *Revista Multidisciplinar do Nordeste Mineiro, 19*(3), 1–21. https://doi.org/10.61164/pma8x695
55. Qi, T., Xing, L., Fang, Z., Zhang, L., Xiao, H., & Wang, L. (2021). Enhanced oxidation of sulfite over a highly efficient biochar-induced silica composite for sulfur resource utilization in magnesia desulfurization. *Journal of Materials Chemistry A, 9*(22), 13288–13296. https://doi.org/10.1039/D0TA10354C
56. Qi, T., Zhang, S., Zhang, J., Li, T., Xing, L., Fang, Z., An, S., Xu, Z., Xiao, H., & Wang, L. (2023). In situ reconstruction of active catalysis sites triggered by chromium immobilization for sulfite oxidation. *Environmental Science & Technology, 57*(9), 3905–3916. https://doi.org/10.1021/acs.est.2c09606 .
57. Qi, T., Zhou, C., Ma, S., Liu, W., Li, T., An, S., Li, Q., Xing, L., & Wang, L. (2026). Dual-site engineered LDHs for concurrent targeted selenium sequestration and high-value sulfur recovery from WFGD byproducts. *Applied Surface Science, 734*, 167047. https://doi.org/10.1016/j.apsusc.2026.167047
58. Ren, C., Wang, W., Hua, D., Wu, S., & Yao, Y. (2021). Preparation and properties of a sulphoaluminate magnesium-potassium phosphate green cementitious composite material from industrial solid wastes. *Materials, 14*(23), 7340. https://doi.org/10.3390/ma14237340
59. Rodrigues, I. N., de Medeiros, J. L., & Araújo, O. de Q. F. (2021). Sulfite removal from flue-gas desulfurization residues of coal-fired power plants: Oxidation experiments and kinetic parameters estimation. *Energy Reports, 7*, 8142–8151. https://doi.org/10.1016/j.egyr.2021.04.062
60. Roshan, N., Battaglia, M., Sau, G. S., Tizzoni, A. C., Veca, E., Corsaro, N., Spadoni, A., D'Auria, M., D'Ottavi, C., Licoccia, S., Lanchi, M., Turchetti, L., & Murmura, M. A. (2026). Sulfur dioxide disproportionation by magnesium sulfite as intermediate. *Processes, 14*(16), 2617. https://doi.org/10.3390/pr14162617
61. Scherman Johansson, S. (2025). WSA, the resilient solution to fluctuating lean SO_2 gases. In The Metallurgy and Materials Society of CIM, The Society for Mining, Metallurgy & Exploration, & The Minerals, Metals & Materials Society (Eds.), *12th International Copper Conference: Proceedings of the Extraction 2025 Meeting & Exhibition, Volume I* (pp. 65–69). Springer. https://doi.org/10.1007/978-3-032-00102-3_7
62. Schmidt, J., & Shang, H. (2026). Reducing copper/nickel smelter SO_2 emissions through enhanced modeling of an associated sulfuric acid plant's dynamics. *Journal of Sustainable Metallurgy, 12*(2), 1377–1389. https://doi.org/10.1007/s40831-025-01388-6
63. Stanienda-Pilecki, K. J. (2021). The use of limestones built of carbonate phases with increased Mg content in processes of flue gas desulfurization. *Minerals, 11*(10), 1044. https://doi.org/10.3390/min11101044
64. Strong, C., Sokhanvaran, S., & Candy, I. (2025). New copper smelter: How to select the right technology and configuration? In The Metallurgy and Materials Society of CIM, The Society for Mining, Metallurgy & Exploration, & The Minerals, Metals & Materials Society (Eds.), *12th International Copper Conference: Proceedings of the Extraction 2025 Meeting & Exhibition, Volume I* (pp. 2397–2428). Springer. https://doi.org/10.1007/978-3-032-00102-3_216
65. Sun, Y., Xie, J., Huang, W., Li, G., Li, S., Cui, P., Xu, H., Qu, Z., & Yan, N. (2021). Novel product-adjustable technology using Wellman-Lord method coupled with sodium-alkali for SO_2 removal and regeneration from smelting gas. *Fuel, 288*, 119714. https://doi.org/10.1016/j.fuel.2020.119714
66. Tang, R., Li, C., Gong, Z., Liu, Y., Li, Y., Ning, H., Gu, X., Jin, Z., & Yu, J. (2024). The effect of magnesium content and roasting process on the structure and desulfurization activity of slaked lime derived from limestone. *Journal of Environmental Chemical Engineering, 12*(4), 113195. https://doi.org/10.1016/j.jece.2024.113195

67. Tang, X.-J., Du, Z.-Y., Zhu, Y.-M., Liu, P.-F., Li, X.-Y., Xu, X.-L., Zhao, Y.-Z., & Kuang, H.-B. (2020). Correlation between microstructure and dissolution property of magnesium hydroxide synthesized via magnesia hydroxylation: Effect of hydration agents. *Journal of Cleaner Production, 249*, 119371. https://doi.org/10.1016/j.jclepro.2019.119371
68. Tang, Z., Wang, Y., Liu, J., Xu, B., Ding, L., Huang, W., Dai, Z., Jiang, W., Yao, L., & Yang, L. (2023). Removal and resource utilization of high concentration flue gas sulfur dioxide using manganese carbonate ore. *Atmosphere, 14*(5), 835. https://doi.org/10.3390/atmos14050835
69. Tao, L., Chen, X., Wang, L., Wang, X., Ning, P., Cai, B., & Pu, Y. (2022). Integration for sulfur dioxide removal from smelting flue gas with copper tailings utilization and copper recovery via absorption-synchronous leaching and reduction. *Environmental Technology & Innovation, 28*, 102931. https://doi.org/10.1016/j.eti.2022.102931
70. Tian, H., Wan, D., Che, Y., Chang, J., Zhao, J., Hu, X., Guo, Q., Wang, Z., & Wang, L. (2021). Simultaneous magnesia regeneration and sulfur dioxide generation in magnesium-based flue gas desulfurization process. *Journal of Cleaner Production, 284*, 124720. https://doi.org/10.1016/j.jclepro.2020.124720
71. Tisdale, D. G., Muinonen, S. J., Molinski, M. D., & Stokreef, A. G. (2021). A novel process to reduce SO_2 emissions during electric furnace smelting of sulphides. In C. Anderson, G. Goodall, S. Gostu, D. Gregurek, M. Lundström, C. Meskers, S. Nicol, E. Peuraniemi, F. Tesfaye, P. K. Tripathy, S. Wang, & Y. Zhang (Eds.), *Ni-Co 2021: The 5th International Symposium on Nickel and Cobalt* (pp. 307–315). Springer. https://doi.org/10.1007/978-3-030-65647-8_26
72. U.S. Environmental Protection Agency. (1981). *Summary report: Sulfur oxides control technology series: Flue gas desulfurization, magnesium oxide process* (EPA-625/8-81-005). Industrial Environmental Research Laboratory. EPA NEPIS — registro oficial
73. von Hoessle, F., Mohamed, M., Farid, R., Hammouda, R. M., Kühn, F. E., & Bassioni, G. (2021). Interfacial phenomena of magnesium hydroxide micro phases. *Ain Shams Engineering Journal, 12*(3), 3133–3140. https://doi.org/10.1016/j.asej.2021.01.020
74. Wang, H., Zhong, C., Ma, Q., Ma, J., & He, H. (2020). The adsorption and oxidation of SO_2 on MgO surface: Experimental and DFT calculation studies. *Environmental Science: Nano, 7*(4), 1092–1101. https://doi.org/10.1039/C9EN01474H.
75. Wang, J., Huang, W., Xu, H., Cui, P., Qu, Z., & Yan, N. (2023). High-efficient cyclic absorption of sulfur dioxide in Na-Mg-Ci^{3-} compound system for wet flue gas desulfurization. *Separation and Purification Technology, 320*, 124138. DOI: 10.1016/j.seppur.2023.124138.
76. Wang, L., Fang, Z., Qi, T., Xing, L., Liu, J., Zhang, S., Xu, P., & Ning, P. (2020). Short-range ordered $Co(OH)_2/TiO_2$ for boosting sulfite oxidation: Performance and mechanism. *Journal of Colloid and Interface Science, 571*, 90–99. DOI: 10.1016/j.jcis.2020.03.042.
77. Wang, Y., Qi, T., Hu, M., Yang, Y., Xing, L., & Wang, L. (2020). Simultaneous catalysis of sulfite oxidation and uptake of heavy metals by bifunctional activated carbon fiber in magnesia desulfurization. *Catalysts, 10*(2), 244. DOI: 10.3390/catal10020244.
78. Weber, P., Behrmann, D., Breuer, T., & Margraf, R. (2020). Installation of a brown field slag reduction furnace: State of the art off-gas treatment with dry gas cleaning for SO_2 capture. In A. Siegmund, S. Alam, J. Grogan, U. Kerney, & E. Shibata (Eds.), *PbZn 2020: 9th International Symposium on Lead and Zinc Processing* (pp. 187–200). Springer. Observação: não encontrei DOI individual confiável para este capítulo. O DOI 10.1007/978-3-030-37070-1 corresponde ao volume, não deve ser apresentado como DOI exclusivo do capítulo. A referência bibliográfica posterior da AIP confirma os quatro autores e pp. 187–200.
79. Weiß, B. D., & Harasek, M. (2021). Solubility data of potential salts in the MgO–CaO–SO_2–H_2O–O_2 system for process modeling. *Processes, 9*(1), 50. DOI: 10.3390/pr9010050.
80. Weiß, B. D., Fuchs, W., & Harasek, M. (2021). Finding optimized process conditions to minimize precipitations in an SO_2 absorption process using thermodynamic process simulation. *Chemical Engineering Transactions, 88*, 535–540. DOI: 10.3303/CET2188089.
81. Weiß, B. D., Haddadi, B., & Harasek, M. (2023). Assessment of modeling the MgO–CaO–CO_2–SO_2–H_2O–O_2 system using the electrolyte NRTL activity coefficient model. *Industrial & Engineering Chemistry Research, 62*(32), 12626–12639. DOI: 10.1021/acs.iecr.3c00868.
82. Weng, W., Zhang, W., Lin, H., Chi, X., & Zhong, S. (2023). Fixing sulfur dioxide by feeding calcine oxide into the rotary volatilization kiln in zinc smelting plant. *Environmental Science and Pollution Research, 30*(15), 43768–43777. DOI: 10.1007/s11356-023-25164-9.
83. Wilailak, S., Yoo, B.-H., Kim, Y. P., & Lee, C.-J. (2021). Parametric analysis and design optimization of wet SOx scrubber system in marine industry. *Fuel, 304*, 121369. DOI: 10.1016/j.fuel.2021.121369.
84. Xie, J., Wang, D., Liu, L., Shao, T., Zhou, H., & Zhang, D. (2024). An overview of flue gas SO_2 capture technology based on absorbent evaluation and

process intensification. *Industrial & Engineering Chemistry Research*, *63*(14), 6066–6086. DOI: 10.1021/acs.iecr.4c00405.

85. Xing, L., Li, M., Qi, T., Mao, L., Hu, Z., Zhang, E., Hao, G.-P., Mao, B., & Wang, L. (2022). Construction of confined bifunctional 2D material for efficient sulfur resource recovery and Hg^{2+} adsorption in desulfurization. *Environmental Science & Technology*, *56*(7), 4531–4541. DOI: 10.1021/acs.est.2c00377.
86. Xing, L., Liu, J., Qi, T., Wang, L., Wang, Z., & Zhang, S. (2020). Superior energy-saving catalyst of Mn@ZIF67 for reclaiming byproduct in wet magnesia desulfurization. *Applied Catalysis B: Environmental*, *275*, 119143. DOI: 10.1016/j.apcatb.2020.119143.
87. Yan, L., Lu, X., Wang, Q., Kang, Y., Xu, J., & Chen, Y. (2014). Research on sulfur recovery from the byproducts of magnesia wet flue gas desulfurization. *Applied Thermal Engineering*, *65*(1–2), 487–494. DOI: 10.1016/j.applthermaleng.2014.01.032.
88. Yan, M., & Shi, Y. (2020). Thermal and economic analysis of multi-effect concentration system by utilizing waste heat of flue gas for magnesium desulfurization wastewater. *Energies*, *13*(20), 5384. DOI: 10.3390/en13205384.
89. Yang, H., Hu, T., Zhao, F., Wang, F., Cui, S., Ning, P., Feng, J., & Jia, L. (2026). Discarded cigarette butt-derived cobalt-based bifunctional catalysts for simultaneous catalytic oxidation of $MgSO_3$ and adsorption of Pb(II) in magnesium-based flue gas desulfurization systems. *Arabian Journal of Chemistry*, *19*(5), 5372025. DOI: 10.25259/AJC_537_2025.
90. Zeng, F., Zhu, J., Liu, F., Zhang, G., Li, W., Li, W., Shang, Z., You, H., Wang, S., & Li, Z. (2025). Bentonite supported cobalt catalyst prepared by blending method for the catalytic oxidation of desulfurization by-product sulfite: Catalytic performance and mechanism. *Journal of Environmental Sciences*, *156*, 584–595. DOI: 10.1016/j.jes.2025.02.032.
91. Zeng, S., Zhu, H., Xia, S., & Yue, B. (2026). A time-frequency dual-branch feature dynamic fusion prediction network for tail gas sulfur content prediction in the wet flue gas desulfurization process. *Engineering Applications of Artificial Intelligence*, *167*, 113865. DOI: 10.1016/j.engappai.2026.113865.
92. Zhang, C., Zou, D., Huang, X., & Lu, W. (2022). Coal-fired boiler flue gas desulfurization system based on slurry waste heat recovery in severe cold areas. *Membranes*, *12*(1), 47. DOI: 10.3390/membranes12010047.
93. Zhang, L., Xing, L., Liu, J., Qi, T., Li, M., & Wang, L. (2021). Synchronous catalysis of sulfite oxidation and abatement of Hg^{2+} in wet desulfurization using one-pot synthesized Co-TUD-1/S. *Separation and Purification Technology*, *266*, 118546. DOI: 10.1016/j.seppur.2021.118546.
94. Zhang, N., Lin, X., Hu, Z., Ding, W., & Zou, J. (2025). Developing advanced Mg-based solid-state materials for gas separation and purification: A review. *Interdisciplinary Materials*, *4*(3), 480–501. DOI: 10.1002/idm2.12250.
95. Zhang, T., He, L., Ou, X., Wang, W., & Wang, D. (2025). UV synergistic magnesium oxide desulfurization waste residue for efficient decoloration of swine wastewater biochemical effluent. *Journal of Water Process Engineering*, *75*, 107912. DOI: 10.1016/j.jwpe.2025.107912.
96. Zhao, L.-D., Zhong, Y.-D., Zhang, R.-L., Zhao, H., & Liu, R.-J. (2025). Study on dispersion stability of natural brucite in aqueous media. *Journal of Dispersion Science and Technology*, *46*(5), 729–737. DOI: 10.1080/01932691.2023.2299345.
97. Zhao, M., & Zou, C. (2021). The effect of particle size on removal of SO_2 from flue gas by MgO absorbents. *Powder Technology*, *377*, 506–513. DOI: 10.1016/j.powtec.2020.08.092.
98. Zhao, Z., Fan, H., Li, Q., Liu, C., Chen, Z., Li, L., Zheng, C., & Gao, X. (2022). Hybrid modeling and operating optimization method of oxidation process of wet flue gas desulfurization (WFGD) system. *Chemical Engineering Research and Design*, *188*, 406–416. DOI: 10.1016/j.cherd.2022.09.045.
99. Zhao, Z., Zhang, Y., Gao, W., Baleta, J., Liu, C., Li, W., Weng, W., Dai, H., Zheng, C., & Gao, X. (2021). Simulation of SO_2 absorption and performance enhancement of wet flue gas desulfurization system. *Process Safety and Environmental Protection*, *150*, 453–463. DOI: 10.1016/j.psep.2021.04.032.
100. Zhao, Z., Zhang, Y., Shao, Y., Liu, C., Li, W., Fan, H., Dai, H., Yang, Y., Zheng, C., & Gao, X. (2022). Simulation of SO_2 removal process from marine exhaust gas by hybrid exhaust gas cleaning systems (EGCS) using seawater and magnesium-based absorbent. *Separation and Purification Technology*, *287*, 120557. DOI: 10.1016/j.seppur.2022.120557.
101. Zheng, X., Li, X., Lei, Y., Zhang, J., Zhai, B., & Li, S. (2025). Development status of flue gas desulfurization processes in smelting and thermal power enterprises. *Clean Coal Technology*, *31*, 527–531. DOI: 10.13226/j.issn.1006-6772.24071802.
102. Zhong, M., Xi, H., Cao, C., Lü, Y., Xiong, F., & Wu, S. (2026). Thermodynamic analysis of wet desulfurization system with a mixture of magnesium sulfite and sodium sulfite. *Nonferrous Metals Science and Engineering*, *17*(1), 47–55.
103. Zhong, Q., Shen, H., Yun, X., Chen, Y., Ren, Y., Xu, H., Shen, G., Du, W., Meng, J., Li, W., Ma, J., & Tao, S. (2020). Global sulfur dioxide emissions and the driving forces. *Environmental Science & Technology*, *54*(11), 6508–6517. DOI: 10.1021/acs.est.9b07696.

104. Zhu, Y., Zhang, Y., Wang, J., Jia, S., Ma, Y., Li, G., Li, X., & Zheng, Q. (2026). Controlled synthesis of $Mg(OH)_2$ with tailored crystal morphologies from brucite via hydration: Morphological evolution mechanism and hydration kinetics. *Journal of Crystal Growth*, *679*, 128501. DOI: 10.1016/j.jcrysgro.2026.128501.